

independent of the technique of surgeons. On the other hand, there is one notable limitation to this system in that the connecting device was directly exposed to blood flow, which might promote thrombus formation at the luminal surface of the device. Because of the small caliber of the grafts, even small thrombi could result in occlusion. However, the early endothelialization promoted by the microporous mesh structure could prevent this complication. Therefore, this system minimizing the blood flow interruption to obtain complete and reliable anastomosis was appropriate for this study.

Conclusion

The biotube vascular grafts provided high patency even when implanted in extremely small-caliber vessels with internal diameter of 1.5 mm. An almost complete artery-like structure with cellular components of endothelial cells and smooth muscle cells and extracellular components of collagen and elastin was formed only 12 weeks after implantation. Biotubes could thus be used as small-caliber vascular prostheses that greatly facilitated the healing process and exhibited excellent biocompatibility.

Acknowledgments The authors thank Ms. Manami Sone for her technical support in this study. This study was funded in part by a Grant-in-Aid for Scientific Research (B23360374) from the Ministry of Education, Culture, Sports, Science and Technology of Japan.

References

- Tomizawa Y. Vascular prostheses for aortocoronary bypass grafting: a review. *Artif Organs*. 1995;19:39–45.
- Ferrari ER, von Segesser LK. Arterial grafting for myocardial revascularization: how better is it? *Curr Opin Cardiol*. 2006;21(6):584–8.
- Faries PL, LoGerfo FW, Arora S, Hook S, Pulling MC, Akbari CM, Campbell DR, Pomposelli FB Jr. A comparative study of alternative conduits for lower extremity revascularization: all-autogenous conduit versus prosthetic grafts. *J Vasc Surg*. 2000;32:1080–90.
- Daenens K, Schepers S, Fourneau I, Hounthoofd S, Nevelsteen A. Heparin-bonded ePTFE grafts compared with vein grafts in femoropopliteal and femorocrural bypass: 1- and 2-year results. *J Vasc Surg*. 2009;49:1210–6.
- Ao PY, Hawthorne WJ, Vicaretti M, Fletcher JP. Development of intimal hyperplasia in six different vascular prostheses. *Eur J Vasc Endovasc Surg*. 2000;20:241–9.
- Isenberg BC, Williams C, Tranquillo RT. Small-diameter artificial arteries engineered in vitro. *Circ Res*. 2006;98(1):25–35.
- Nakayama Y, Ishibashi-Ueda H, Takamizawa K. In vivo tissue-engineered small-caliber arterial graft prosthesis consisting of autologous tissue (biotube). *Cell Transpl*. 2004;13:439–49.
- Watanabe T, Kanda K, Ishibashi-Ueda H, Yaku H, Nakayama Y. Development of biotube vascular grafts incorporating cuffs for easy implantation. *J Artif Organs*. 2007;10:10–5.
- Sakai O, Kanda K, Ishibashi-Ueda H, Takamizawa K, Ametani A, Yaku H, Nakayama Y. Development of the wing-attached rod for acceleration of “Biotube” vascular grafts fabrication in vivo. *J Biomed Mater Res B Appl Biomater*. 2007;83:240–7.
- Watanabe T, Kanda K, Ishibashi-Ueda H, Yaku H, Nakayama Y. Autologous small-caliber “Biotube” vascular grafts with argatroban loading: a histomorphological examination after implantation to rabbits. *J Biomed Mater Res B Appl Biomater*. 2010;92:236–42.
- Watanabe T, Kanda K, Yamanami M, Ishibashi-Ueda H, Yaku H, Nakayama Y. Long-term animal implantation study of biotube—autologous small-caliber vascular graft fabricated by in-body tissue architecture. *J Biomed Mater Res B Appl Biomater*. 2011;98(1):120–6.
- Hayashida K, Kanda K, Yaku H, Ando J, Nakayama Y. Development of an in vivo tissue-engineered, autologous heart valve (the biovalve): preparation of a prototype model. *J Thorac Cardiovasc Surg*. 2007;134:152–9.
- Yamanami M, Yahata Y, Uechi M, Fujiwara M, Ishibashi-Ueda H, Kanda K, Watanabe T, Tajikawa T, Ohba K, Yaku H, Nakayama Y. Development of a completely autologous valved conduit with the sinus of Valsalva using in-body tissue architecture technology: a pilot study in pulmonary valve replacement in a beagle model. *Circulation*. 2010;122:S100–6.
- Sakai O, Nakayama Y, Nemoto Y, Okamoto Y, Watanabe T, Kanda K, Yaku H. Development of sutureless vascular connecting system for easy implantation of small-caliber artificial grafts. *J Artif Organs*. 2005;8:119–24.
- Lopez-Soler RI, Brennan MP, Goyal A, Wang Y, Fong P, Tellides G, Sinusas A, Dardik A, Breuer C. Development of a mouse model for evaluation of small diameter vascular grafts. *J Surg Res*. 2007;139:1–6.
- Narita Y, Kagami H, Matsunuma H, Murase Y, Ueda M, Ueda Y. Decellularized ureter for tissue-engineered small-caliber vascular graft. *J Artif Organs*. 2008;11:91–9.
- Pektok E, Nottelet B, Tille JC, Gurny R, Kalangos A, Moeller M, Walpoth BH. Degradation and healing characteristics of small-diameter poly(epsilon-caprolactone) vascular grafts in the rat systemic arterial circulation. *Circulation*. 2008;118:2563–70.
- Shin'oka T, Imai Y, Ikada Y. Transplantation of a tissue-engineered pulmonary artery. *N Engl J Med*. 2001;15:532–3.
- Campbell JH, Efendy JE, Campbell GR. Novel vascular graft grown within recipient's own peritoneal cavity. *Circ Res*. 1999;85:1173–8.
- Watanabe T, Kanda K, Yamanami M, Yaku H, Nakayama Y. Biotubes designed for large animals: auto-implantation to the carotid artery of the beagle dogs. *Int J Artif Organs*. 2008;31:601.
- Watanabe T, Yamanami M, Kanda K, Ishibashi-Ueda H, Yaku H, Nakayama Y. Application of biotube vascular grafts to abdominal region in a beagle model. *Int J Artif Organs*. 2010;33:466.
- Shindo S, Takagi A, Whittemore AD. Improved patency of collagen-impregnated grafts after in vitro autogenous endothelial cell seeding. *J Vasc Surg*. 1987;6:325–32.
- Kuwabara F, Narita Y, Yamawaki-Ogata A, Kanie K, Kato R, Satake M, Kaneko H, Oshima H, Usui A, Ueda Y. Novel small-caliber vascular grafts with trimeric Peptide for acceleration of endothelialization. *Ann Thorac Surg*. 2012;93(1):156–63.
- Hibino N, Villalona G, Pietris N, Duncan DR, Schoffner A, Roh JD, Yi T, Dobrucki LW, Mejias D, Sawh-Martinez R, Harrington JK, Sinusas A, Krause DS, Kyriakides T, Saltzman WM, Pober JS, Shin'oka T, Breuer CK. Tissue-engineered vascular grafts form neovessels that arise from regeneration of the adjacent blood vessel. *FASEB J*. 2011;25(8):2731–9.
- Yamanami M, Yamamoto A, Iida H, Watanabe T, Kanda K, Yaku H, Nakayama Y. 3-Tesla magnetic resonance angiographic assessment of a tissue-engineered small-caliber vascular graft implanted in a rat. *J Biomed Mater Res B Appl Biomater*. 2010;92:156–60.

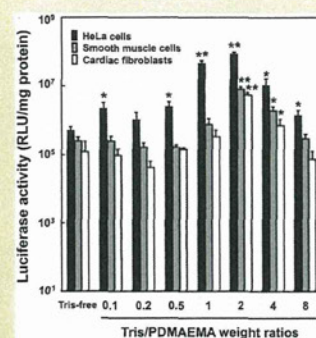
Enhanced Transfection Efficiency of Poly(*N,N*-dimethylaminoethyl methacrylate)-Based Deposition Transfection by Combination with Tris(hydroxymethyl)aminomethane

Ryosuke Iwai,[†] Ryota Haruki,[†] Yasushi Nemoto,^{†,‡} and Yasuhide Nakayama^{*,†}

[†]Division of Medical Engineering and Materials, National Cerebral and Cardiovascular Center Research Institute, Japan

[‡]Development Department, Chemical Products Division, Bridgestone Co., Japan

ABSTRACT: We have developed a substrate-mediated transfection method called “deposition transfection technology” using a poly(*N,N*-dimethylaminoethylmethacrylate) (PDMAEMA) homopolymer with both thermoresponsive and cationic characteristics. In this study, we enhanced deposition transfection efficiency by using tris(hydroxymethyl)aminomethane (Tris buffer) as a pH adjuster for transfection solution composed of PDMAEMA and plasmid DNA (pDNA). PDMAEMA with a molecular weight of 9.7×10^4 g mol⁻¹ was synthesized by photoinduced radical polymerization. The pH of PDMAEMA solution was increased gradually in the range from 8 to 11 by the addition of Tris, and then the solubility of PDMAEMA was significantly decreased and the dissolution time was extended from 15 to 40 min at Tris/PDMAEMA ratio of 1 and higher. On the other hand, while the polyion complexes (polyplexes) were formed by mixing PDMAEMA with luciferase-encoding plasmid DNA even under an excess amount of Tris at Tris/PDMAEMA ratio of 8, the binding affinity between PDMAEMA and pDNA was decreased with increasing Tris at Tris/PDMAEMA ratio of 2 and higher. When HeLa cells, smooth muscle cells, and cardiac fibroblasts were transfected by the deposition method using polyplex solution containing various amounts of Tris, the transgene expression dramatically increased at a Tris/PDMAEMA ratio of 2 in all cell types, which were more than 150-fold in HeLa cells, 40-fold in smooth muscle cells, and 30-fold in cardiac fibroblasts compared to those in the Tris-free condition. In addition, the enhanced transgene expression by Tris was sustained for over 10 days post-transfection as well as that observed in Tris-free condition. Thus, deposition transfection efficiency can be dramatically enhanced by using Tris buffer as a pH adjuster for polyplex solution.



INTRODUCTION

Controlled gene delivery to specific tissues or cells (targeted transfection) and enhancement of transfection activity are important in fields such as regenerative medicine and gene therapy.^{1,2} For the development of controlled transfection technology, nonviral gene carriers such as synthetic cationic polymers and cationic liposomes are considered promising transfection reagents because, in contrast to viral vectors, they are easily able to deliver a diverse set of functional molecules such as signal peptides,^{3,4} bioactive molecules,^{5,6} thermoresponsive molecules,^{7,8} or pH responsive molecules.^{9,10}

With this in mind, we developed a novel surface-mediated transfection technology called “deposition transfection” that allowed us to obtain high and sustained transgene expression of plasmid DNA (pDNA) deposited on culture surface, treated by using surfactant polymers for the thermoresponsive surface immobilization of pDNA.^{8,11} For the first-generation deposition transfection reagent, we designed a polymer comprising 4 AB-type block branches: a cationic poly(*N,N*-dimethylaminopropylacrylamide) (PDMAPAAM) block and a thermoresponsive poly(*N*-isopropylacrylamide) (PNIPAM) block (PDMAPAAM-PNIPAM).⁸ This polymer could form polyion complexes (polyplexes) with pDNA and get deposited on a cell culture surface at 37 °C. Transgene expression from this plasmid was observed in cells seeded on this culture surface. Next, we

prepared a second-generation reagent by focusing on poly(*N,N*-dimethylaminoethylmethacrylate) (PDMAEMA), which is a homopolymer with both cationic and thermoresponsive characteristics. By using PDMAEMA, we significantly reduced the amount of polymer required to produce the polyplexes of polymer with pDNA. In fact, we observed a 25% reduction compared to the amounts required for our previous PDMAPAAM-PNIPAM block copolymer. Compared with the use of commercially available Lipofectamine2000, by using PDMAEMA, we also obtained significantly higher transfection efficiency and cell viability in cell lines and primary cells.¹¹ Despite this, the transfection efficiencies for primary cells such as cardiac fibroblasts and smooth muscle cells were still lower compared to that obtained using cell lines such as HeLa and Cos-1. Therefore, the application of PDMAEMA deposition transfection technology in many fields such as artificial organ, regenerative medicine, and gene therapy is preferable for the enhancement of transfection efficiency toward primary cells.

The processes of cellular uptake, endosomal escape, cytoplasmic transport, nuclear entry, and disassembly of polyplexes are considered typical barriers for polymer-mediated

Received: June 15, 2012

Revised: January 13, 2013

Published: January 29, 2013

gene delivery.¹² Therefore, many multifunctional intelligent polymers have been synthesized to overcome these barriers.^{13–15} On the other hand, Kang et al. focused on the effect of environmental pH, that is, the pH values of polyplex solution, transfection medium, and culture medium on transfection efficiency using cationic polymer, because the environmental pH could affect the characteristics of a polymer and how it polyplexes with pDNA and affects target cell physiology.¹⁶ Further, PDMAEMA is protonated (cationic) at low pH (<7), and deprotonated at high pH (>8) (completely neutral at pH = 10).¹⁷ Therefore, the pH of PDMAEMA solution might affect the particle size, complex formation/deformation potential, and surface charge of its polyplexes with pDNA. Alterations in these parameters can then potentially affect the efficiency of cellular uptake, endosomal escape, cytoplasmic transport, and nuclear entry of polyplexes. However, the effects of pH on the characteristics of polyplexes of PDMAEMA with pDNA and its transfection activity have not been examined. To our knowledge, there is also no report that addresses the effect of the pH of polyplex solutions on substrate-mediated transfection technologies.

Tris(hydroxymethyl)aminomethane (Tris) is one of the most useful buffering agents that rapidly restores pH and acid–base regulation, and therefore, it has been extensively used not only in basic research fields of biochemistry and molecular biology as the buffer solutions for DNA, RNA, and proteins, but also in clinical practices for diabetic or renal acidosis and metabolic acidosis associated with cardiac bypass surgery or cardiac arrest.^{18,19} Tris is a compound with basic property (pH = 11 at 10 mM) having an effective pH range between 7.0 and 9.0. Its pH can be easily controlled by titration with HCl (Tris-HCl acid salt) for use in many experimental purposes including transfection experiments. Here, we suggest that the characteristics of PDMAEMA such as thermoresponsibility, particle size, and complexation/decomplexation of its polyplexes with pDNA could be controlled and optimized for enhancing transfection by changing solution pH by using Tris buffer as a safety pH adjuster. Therefore, in this study, we examined the effects of Tris addition on the thermoresponsive nature of PDMAEMA and the characteristics of its polyplexes with pDNA. We then determined the optimal Tris additive amount for enhancing deposition transfection efficiency of PDMAEMA.

EXPERIMENTAL SECTION

General Methods. ¹H NMR spectra were recorded using a 300 MHz NMR spectrometer (Gemini 300; Varian, Palo Alto, CA) with chloroform-*d*₁ at room temperature. Gel permeation chromatography (GPC) analyses using *N,N*-dimethylformamide as a solvent were carried out using an HPLC-8320 GPC instrument (Tosoh, Tokyo, Japan) in conjunction with Tosoh TSKgel SuperAW-4000 and SuperAW-5000 columns. The columns were calibrated prior to use by using narrow distribution poly(ethylene glycol) standards (Tosoh).

Synthesis and Thermoresponsive Characters of PDMAEMA. Poly(*N,N*-dimethylaminoethylmethacrylate) (PDMAEMA) was synthesized according to the procedure given in our previous report.¹¹ Briefly, DMAEMA (7.0 g, Tokyo Kasei Co., Tokyo, Japan) was poured into a glass tube (35 × 65 mm, Maruemu Co., Osaka, Japan) under N₂ gas atmosphere. DMAEMA was irradiated for 21 h by using an 18 W fluorescent light (FCL20BL; NEC Co., Tokyo, Japan). After irradiation, reprecipitation was carried out 6 times with chloroform solution in hexane (Kanto Chemical Co., Tokyo,

Japan). The final precipitate was dried under reduced pressure, following which, PDMAEMA was obtained (4.3 g, 61.4% conversion). The molecular weight of PDMAEMA was determined to be 9.7×10^4 g·mol⁻¹ (polydispersity: 4.1) by GPC analysis. ¹H NMR: δ 0.8–1.2 ppm (br, -CH₃), 1.6–2.0 (br, -CH₂-CH₃), 2.2–2.4 (br, N-CH₃), 2.5–2.7 (br, CH₂-N), 4.0–4.2 (br, O-CH₂).

The lower critical solution temperature (LCST) of aqueous solutions of PDMAEMA (1 mg/mL) mixed with different concentrations of tris(hydroxymethyl)aminomethane (Tris; Wako Pure Chemical Ind. Ltd., Osaka, Japan) (0.5–8.0 mg/mL) was determined using a UV–visible spectrophotometer under a heating rate of 0.5 °C/min (UV-1700; Shimadzu, Japan). After complete precipitation of PDMAEMA at 37 °C, the solubility of the PDMAEMA solid in an aqueous Tris solution was observed at 20 °C by optical transmittance change using the UV–visible spectrophotometer.

Surface Analysis. Surface deposition of the PDMAEMA molecules were semiquantitated by surface analysis using attenuated total reflection Fourier transformed infrared spectrometer (FTIR-ATR, IR Pretige-21; Shimadzu, Kyoto, Japan). Briefly, the 100 μL of PDMAEMA solutions (260 μg/mL) containing different amounts of Tris with 0.5- and 2.0-fold weight volume for PDMAEMA were added on the surfaces of cell culture polystyrene plates (Asahi Glass Co., Ltd., Tokyo, Japan). After incubation at 37 °C for 6 h, the surfaces was washed with saline at 20 °C and the absorption spectra from 2600 to 1500 cm⁻¹ on these culture surfaces were acquired by FT-IR spectrometry.

Preparation and Characterization of Polyplexes. PDMAEMA was dissolved in saline (100 μg/mL), and then Tris was added to the solution in 0.1–8.0-fold weight volume for PDMAEMA. Aliquots (60 μL) were added to firefly luciferase-encoding plasmid DNA (33 μg/mL, pGL3 control plasmid; Promega, WI) dissolved in 90 μL of DNase-free pure water (Invitrogen, CA) or Tris-HCl-EDTA buffer (pH 8, Wako) to obtain polymer/pDNA ratios, corresponding to cation/anion (C/A) ratio of 8. The solutions (total volume, 150 μL) were mixed using a pipet to prepare polyplexes.

Polyplexes at the same concentration employed for transfection were used for the mean diameter measurement and DNA gel shift assay. The mean diameter of the polyplexes was determined by dynamic light scattering (DLS) on Zetasizer Nano S (Malvern Instruments Ltd., Worcestershire, UK) equipped with a 10 mW He–Ne laser. For the Tris competitive DNA binding assay, 10 μL aliquots of the polyplexes and DNA solutions were incubated for 30 min at 37 °C and loaded into a 1.2% (w/v) agarose gel slab. The gel was electrophoresed at 100 V for 40 min in 1 × TAE buffer (Wako), including 0.05% ethidium bromide (Wako), and imaged using a UV transmitter (Gel Doc XR System; BIO-RAD, CA).

Primary Cell Culture. Beagles, weighing approximately 10 kg, were humanely used in this experiment according to the Principles of Laboratory Animal Care (formulated by the National Institutes of Health, Publication No. 56–23, received in 1985). Cardiac fibroblasts were isolated from beagle heart ventricles. Briefly, the ventricles were separated and minced into small pieces and digested using 0.25% trypsin solution (Invitrogen, CA) at 37 °C for 1 h with gentle agitation. After filtering the digest through a 100 μm nylon mesh (BD Biosciences, NJ) and centrifugation at 1300 rpm for 3 min, the cell pellet was collected. Following resuspension in Dulbecco's modified Eagle's medium (DMEM) (Gibco, Invitrogen Corp.,

Carlsbad, CA) containing 10% fetal bovine serum (Hyclone Laboratories Inc., Logan, UT), penicillin (200 U/mL; ICN Biomedicals Inc., Aurora, OH), and streptomycin (200 mg/mL; ICN) (growth medium), the cells were placed on a dish (55 cm²; Asahi Glass Co., Ltd.) with the growth medium and cultured in an atmosphere of 5% CO₂ at 37 °C. Aorta smooth muscle cells were isolated from beagle thoracic aortas by modifying the method described previously by Franzblau et al.²⁰ Briefly, the endothelial cell layer of an aorta was removed using a cotton swab. De-endothelialized aorta was minced with scissors into small pieces and digested using a solution containing 0.1% collagenase Type I (Wako) and 0.01% elastase (Wako) at 37 °C for 1 h with gentle agitation. After filtering the digest through a 100 μm nylon mesh, the cells were collected and cultured by the method described above. When the cultures were nearly confluent, cells were harvested and subcultivated at 1.0 × 10⁴ cells/cm².

Green fluorescence (GFP) expressing-adipose derived stromal cells (ADSCs) were isolated from GFP transgenic Lewis rat by a method described in our previous report.¹¹ Briefly, approximately 10 g of fat tissue was harvested from the subcutaneous layer of hind limb and digested using 0.1% collagenase type I solution (Wako) at 37 °C for 1 h with gentle agitation. After filtering the digest through a 100 μm nylon mesh and centrifuging it at 1300 rpm for 3 min, the cell pellet was collected and cultured by the method described above. All cells were used for experiments before they reached the fifth passage.

Transfection to Cell Line and Primary Cells. Transfection by the deposition transfection method was performed as reported previously.¹¹ Briefly, an aqueous solution of the DNA complexes (50 μL; plasmid concentration, 20 μg/mL) was diluted with 150 μL of saline and then added into each well of a 24-well dish (amount of DNA added to each well, 1.0 μg). After incubation at 37 °C for 6 h, HeLa cells, cardiac fibroblasts, smooth muscle cells, ADSCs in 1.0 mL of growth medium were seeded at a density of approximately 5.0 × 10⁴ cells/cm² and cultured in an atmosphere of 5% CO₂ at 37 °C for 2–10 days. The luciferase expression of cells transfected with pGL3 control plasmid was analyzed using a luciferase assay as follows. After 2–10 days of cultivation, the cells were lysed with 0.2 mL of cell lysis buffer (Promega). The lysate was centrifuged at 15 000 rpm for 3 min at 4 °C, and 20 μL of the supernatant was analyzed for luciferase activity by using a Luminus CT-9000 luminometer (Dia-Iatron, Tokyo, Japan). Relative light units (RLU) measurements were standardized using the total protein amounts of the cell lysates, which were determined with BioRad protein assays (BIO-RAD, Hercules, CA) using bovine serum albumin as the standard.

Observation of Cellular Uptake of Polyplexes. Cellular uptake of the polyplexes was observed by using fluorescently labeled plasmid DNA (Label IT plasmid delivery control-Cy3, Mirus, WI, USA). Polyplexes of Cy3-labeled plasmid DNA and PDMAEMA were deposited followed by cell seeding as described above. After 3 days of cell seeding, the cells were washed twice with PBS (-) and polyplexes were visualized by fluorescent microscope (IX71; OLYMPUS, Tokyo, Japan).

Cell Viability Assays. Cytotoxicity was assessed by performing a cell viability assay using the water-soluble tetrazolium (WST)-8 method (Dojindo, Kumamoto, Japan). Polyplex solutions containing different amounts of Tris at Tris/PDMAEMA ratios from 1 to 8 were added to each well in a 96-well plate (Asahi Glass Co. Ltd.). After incubating at 37 °C for

6 h, HeLa cells, cardiac fibroblasts, or smooth muscle cells in 100 μL of the growth medium were seeded (approximately 1.5 × 10⁴ cells per well) and cultured for 24 h at 37 °C in a 5% CO₂ atm. To each well, 10 μL of WST-8 reagent (5 mmol/L) was added. After 2 h incubation at 37 °C, the absorbance at 450 nm was determined using a Bio-Rad microplate reader (model 680; Bio-Rad laboratories Inc., CA, USA).

RESULTS

Thermoresponsive Properties of PDMAEMA. Because PDMAEMA is a slightly cationic polymer, the pH of an aqueous solution of PDMAEMA was approximately 8 (Figure 1). Upon addition of Tris into the PDMAEMA solution, its pH

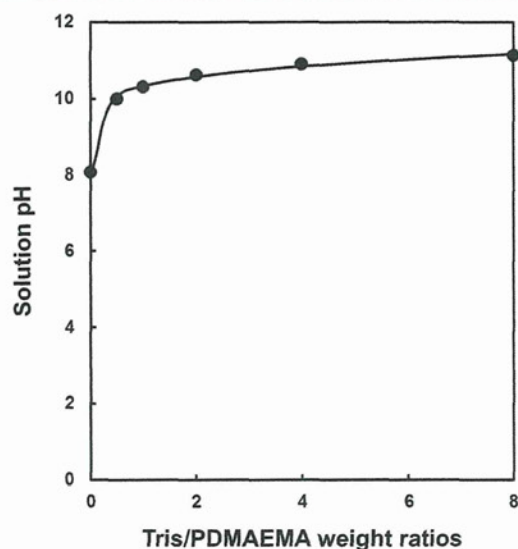


Figure 1. Changes in the PDMAEMA solution pH by the addition of Tris with various amounts. Concentration of PDMAEMA solution: 0.1 mg/mL.

increased gradually, reaching pH 11 in the presence of excess Tris. In addition, we determined that PDMAEMA was thermoresponsive, and its LCST was approximately 26 °C (Figure 2). The LCST was relatively unchanged upon addition of Tris. On the other hand, the solubility of PDMAEMA decreased markedly as the amount of Tris increased (Figure 3). Specifically, PDMAEMA completely dissolved within approximately 15 min, while the dissolution time was extended to 40 min at Tris/PDMAEMA ratios of 2 and above. Thus, the solubility of PDMAEMA in water is inhibited by the presence of Tris.

The PDMAEMA with or without Tris was coated on the culture surface. Upon washing with saline at 20 °C FTIR-ATR absorption signal at 1730 cm⁻¹, originated from C=O stretching vibration of the ester group in PDMAEMA, clearly detected on the PDMAEMA surface coated with Tris, while there was little absorption signal except for 1600 cm⁻¹, originated from C=C bonds of the aromatic hydrocarbons of the polystyrene culture surface, on the Tris-free surface (Figure 4). The adsorption signal level of the PDMAEMA increased with the amount of Tris. Therefore, Tris was effective for the stable deposition of the PDMAEMA on the culture surface.

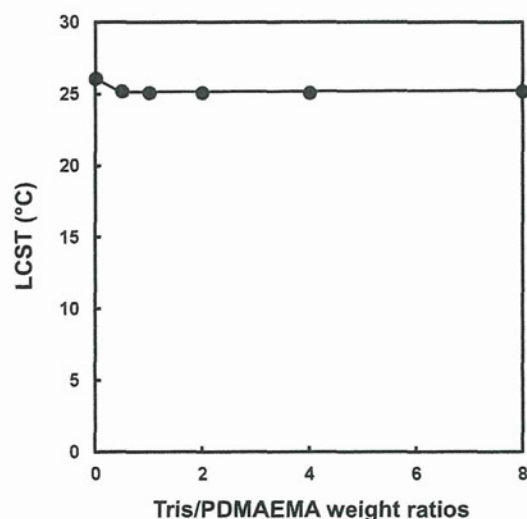


Figure 2. Effect of Tris addition on the LCST of PDMAEMA solution. Concentration of PDMAEMA: 1.0 mg/mL.

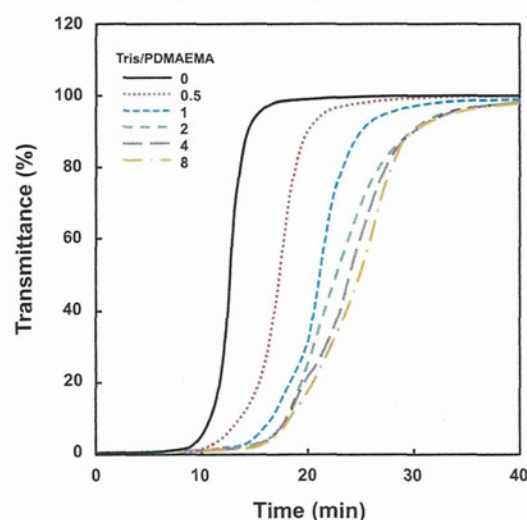


Figure 3. Time course of the transmittance of PDMAEMA solutions containing various amounts of Tris. The PDMAEMA solution was once heated at 37 °C, and then the transmittance was measured at 20 °C. Concentration of PDMAEMA solution: 10 mg/mL.

Polyplex Formation and Stability. The diameter of PDMAEMA particles in water was approximately 72 ± 4 nm. Mixing an aqueous PDMAEMA solution and an aqueous DNA (pGL3 control plasmid) solution leads to immediate formation of PDMAEMA/DNA polyplexes, as demonstrated in our previous report. The diameter of the polyplexes formed at 20 °C under C/A ratio of 8 without Tris was 149.1 ± 10.4 nm (Figure 5). Upon warming at 37 °C, the diameter increased slightly to 158.4 ± 0.5 nm. A similar tendency was observed even in the presence of Tris at a Tris/PDMAEMA weight ratio ranging from 1 to 4. The polyplexes formed in Tris-HCl buffer solution (pH 8, Tris/PDMAEMA ratio of 18) were slightly larger than those formed polyplexes. However, a significant increase in particle diameter occurred in the presence of excess Tris (Tris/PDMAEMA ratio of 8) at both 20 and 37 °C.

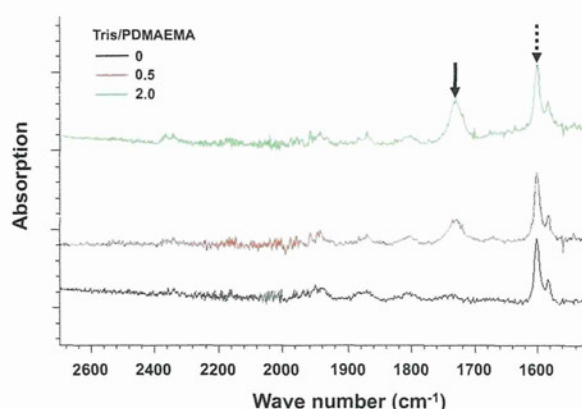


Figure 4. FTIR-ATR spectra of polystyrene culture surfaces coated with PDMAEMA solutions containing different amounts of Tris. Closed and dashed arrows indicate the absorption signals of C=O bonds originated from PDMAEMA and C=C bonds originated from polystyrene, respectively.

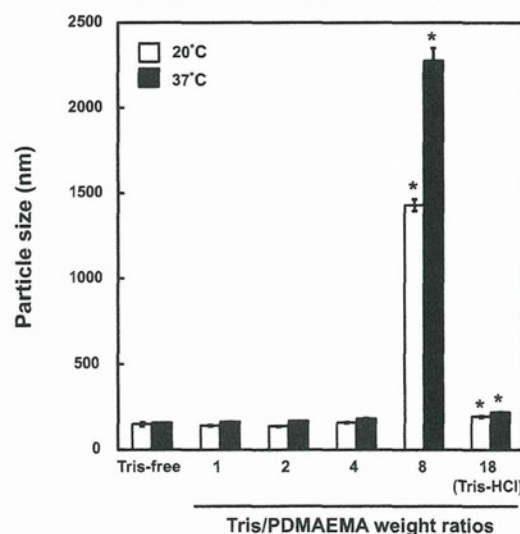


Figure 5. Effect of Tris addition on particle size of the polyplexes prepared by mixing PDMAEMA and pGL3-control plasmid DNA (C/A ratio: 8) at 20 °C (□) and 37 °C (■). The values represent the mean \pm SD ($n = 3$). * $P < 0.05$ relative to Tris-free conditions (control).

The stability of the polyplexes in the presence of Tris was evaluated using an electrophoretic gel shift assay (Figure 6). No free plasmid DNA bands were observed from polyplex preparations dissolved in Tris-free, Tris/PDMAEMA weight ratio of 1, and Tris-HCl buffer solutions. This indicates that, under these conditions, DNA was fully associated with PDMAEMA. On the other hand, bands of DNA did appear in the presence of Tris in solutions with a Tris/PDMAEMA weight ratio of 2 and higher. The intensity of the band was proportional to the Tris/PDMAEMA weight ratio. This demonstrated that the interaction between DNA and PDMAEMA was inhibited by Tris.

Deposition Transfection Study. HeLa cells or primary cardiac fibroblasts and smooth muscle cells were transfected by deposition transfection (see Methods). In HeLa cells, the luciferase expression at 2 days post transfection increased

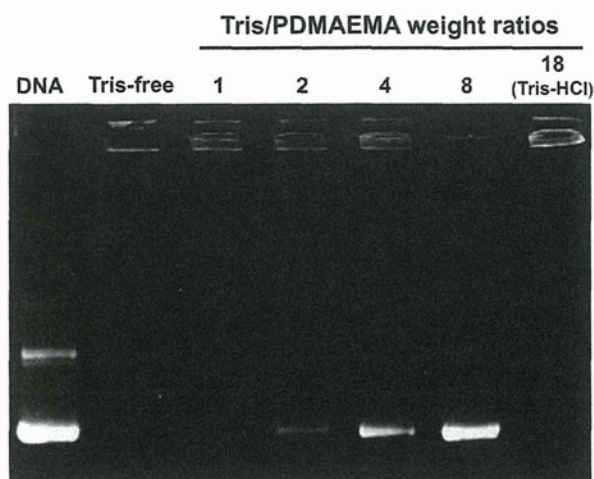


Figure 6. Electrophoretic gel shift assay of the polyplexes of PDMAEMA with pGL3-control plasmid DNA containing various amounts of Tris.

steadily until a Tris/PDMAEMA ratio of 2 was reached, after which it decreased drastically. At the optimal Tris/PDMAEMA ratio of 2, the luciferase activity was more than 150 times that observed in Tris-free conditions. On the other hand, in primary cells, a slight increase in the luciferase expression was observed in the presence of Tris below a Tris/PDMAEMA ratio of 1. However, at a Tris/PDMAEMA ratio of 2, the highest luciferase expression was obtained; compared to Tris-free conditions, there was a 40-fold and 30-fold increase in the activity of the cardiac fibroblasts and smooth muscle cells, respectively.

Consistent with our previous report, elevated luciferase expression was maintained in HeLa cells, smooth muscle cells, and cardiac fibroblasts transfected using the polyplexes for up to 10 days post transfection (Figure 8). The presence of Tris both accelerated and significantly enhanced the luciferase expression—over 50-fold, 55-fold, and 14-fold increases in the luciferase activity of HeLa cells, smooth muscle cells, and cardiac fibroblasts, respectively, compared to those of Tris-free conditions in this observation period.

The cellular uptake of polyplexes was examined by using Cy3-labeled fluorescence plasmid DNA. Figure 9 shows a fluorescence micrograph of the culture surfaces where the GFP-expressing ADSCs were undergoing transfection following the polyplexes of Cy3-labeled plasmid DNA and PDMAEMA were deposited. The weak and blurred red fluorescence signals were observed on the polyplexes-deposited culture surfaces without seeding any cells (Figure 9A), which implies that the red fluorescence derived from Cy3-labeled plasmid DNA were shield by the excess amount of PDMAEMA at C/A ratio of 8. On the other hand, after 72 h of cell seeding, red fluorescence was clearly observed in the cytoplasm of the cells as nanoparticles (Figure 9B), which indicated the uptake of polyplex particles by the cells. When the cells were seeded on the polyplex-deposited surfaces containing Tris at Tris/PDMAEMA weight ratio of 2, which corresponded to the Tris/PDMAEMA ratio that the highest transgene expression was obtained, the numbers of intracellular red nanoparticles were significantly increased compared to that observed in the cells seeded on the surfaces where Tris-free polyplexes were deposited (Figure 9C).

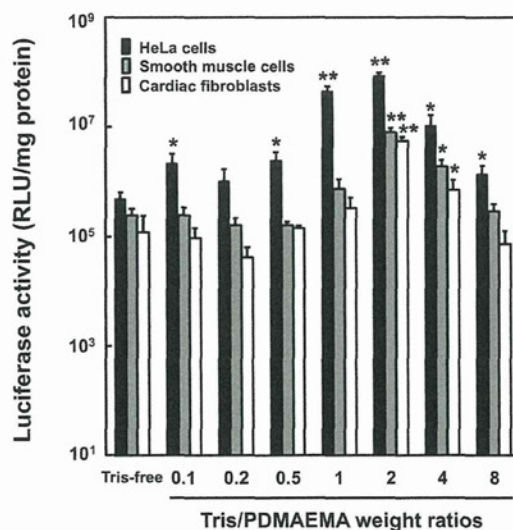


Figure 7. Effect of Tris addition on transgene levels of HeLa cells, smooth muscle cells, and cardiac fibroblasts transfected by deposition method using polyplexes of PDMAEMA with pGL3-control plasmid DNA containing various amounts of Tris. The values represent the mean \pm SD ($n = 3$). * $P < 0.05$, ** $P < 0.01$ relative to Tris-free conditions (control).

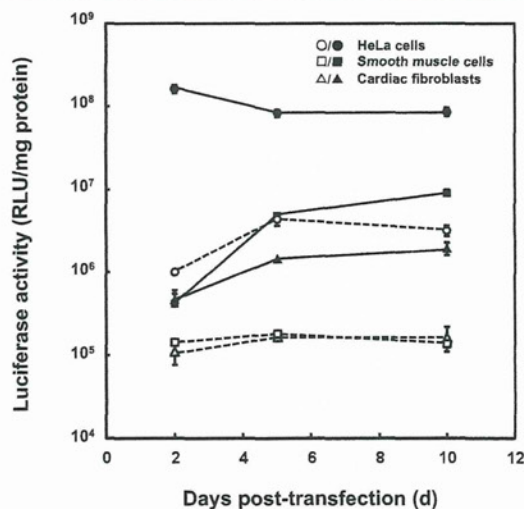


Figure 8. Time course of the luciferase expression levels of HeLa cells (○/●), smooth muscle cells (□/■), and cardiac fibroblasts (△/▲) transfected using polyplexes solution of PDMAEMA with pGL3-control plasmid DNA containing Tris at Tris/PDMAEMA weight ratio of 2 (filled symbol) and without Tris (open symbol and dashed line). The values represent the mean \pm SD ($n = 3$).

The viability of the cells transfected using polyplex solution containing Tris was evaluated for Tris/PDMAEMA ratios from 1 to 8 (Figure 10). In accordance with our previous study,¹¹ high viabilities greater than 90% were obtained in HeLa cells by PDMAEMA-based deposition transfection, and which were not significantly changed by the addition of Tris for any Tris/PDMAEMA weight ratios ($P > 0.05$). Similar to HeLa cells, the viabilities of primary cells such as smooth muscle cells and cardiac fibroblasts were not significantly changed by the addition of Tris, even though those of the smooth muscle

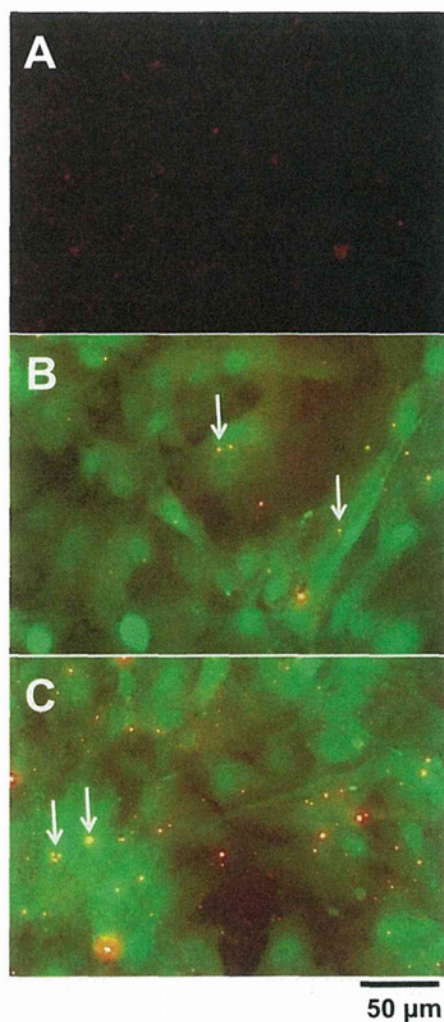


Figure 9. (A) Fluorescence microscopy images of the culture surfaces where the polyplexes of Cy3-labeled plasmid DNA and PDMAEMA were deposited. Fluorescence microscopy images of GFP-expressing adipose-derived stromal cells (ADSCs) undergoing the deposition transfection using the polyplex solution without containing Tris (B) and containing Tris at Tris/PDMAEMA ratio of 2 (C). Polyplex solutions (C/A = 8) were incubated on the culture surfaces for 6 h followed by cell seeding. Images were captured 72 h after cell seeding. Green and red indicate the GFP fluorescence of ADSCs and Cy3 fluorescence of plasmid DNA, respectively. Ten regions of interest were analyzed in two independent experiments.

cells and cardiac fibroblasts were a little lower than that of the HeLa cells. These results indicating that the Tris addition has a little effect on the cytotoxicity of PDMAEMA-based deposition transfection.

DISCUSSION

In this report, we evaluated the suitability of PDMAEMA, a widely used cationic polymer, for use in delivery of DNA via the substrate-mediated deposition transfection method. Since PDMAEMA is a typical cationic polymer, it is used widely as a nonviral gene delivery carrier. In addition to its cationic properties, PDMAEMA is also a thermoresponsive polymer with a low LCST that ranges from 34 to 37 °C.²¹ This unique

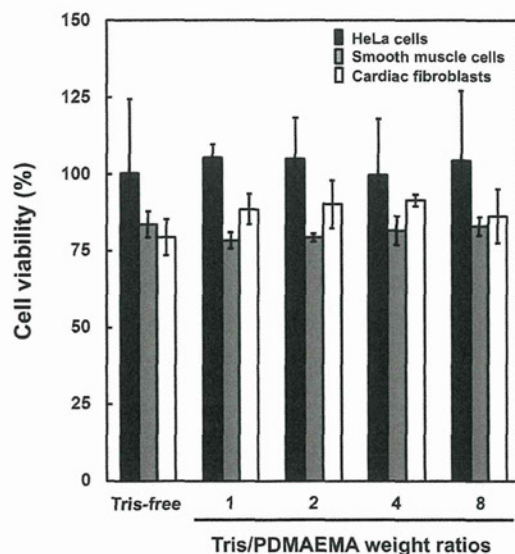


Figure 10. Cytotoxicity of polyplexes prepared by mixing pGL3 control plasmid DNA and PDMAEMA solution containing Tris at different Tris/PDMAEMA weight ratios. The values represent the mean \pm SD ($n = 3$).

combination of properties makes PDMAEMA suitable for bioconjugation with DNA for polyplex formation and amenable to conversion to a water-insoluble form for deposition of polyplexes on a culture dish surface. However, very little biomedical research has been carried out on the dual characteristics of this polymer. In our previous study, we achieved significantly higher transfection efficiency and cell viability by using the deposition transfection method compared with the conventional transfection method using Lipofectamine 2000.¹¹ Our deposition transfection technique is highly suitable for application in fields such as artificial organ biosynthesis, tissue engineering, regenerative medicine, and gene therapy.

In this study, we showed that the Tris base enhanced the efficiency of the deposition transfection method in primary cardiac fibroblasts and smooth muscle cells without Tris dosage-dependent cytotoxicity (Figures 7 and 10). In this method, deposition of the polyplexes from PDMAEMA and DNA onto the culture surface is the most essential step; this in turn is dependent on the thermoresponsive character of PDMAEMA. At low PDMAEMA:DNA ratios, deposition is unstable. On the contrary, high PDMAEMA:DNA ratios result in significant deposition of DNA on the culture dishes, but the surface is coated with a lot of PDMAEMA. In both cases, this can lead to inhibition of transgene expression. Therefore, we set the cation/anion (C/A) ratio to 8, since we found this was optimal from our preliminary study. We reasoned that, if a higher robust deposition could be obtained at the constant C/A ratio of 8, transgene expression would be further increased. As shown in Figure 3, the solubility of PDMAEMA at 20 °C was markedly decreased as the concentration of Tris increased, and the dissolution time was extended from 15 to 40 min at Tris/PDMAEMA ratios of 2 and more. However, the LCST remained constant independently of Tris concentration (Figure 2). Moreover, the increased amount of deposited PDMAEMA on the culture surfaces was confirmed by FTIR-ATR analysis in a Tris dosage-dependent manner (Figure 4). Therefore, we

concluded that the most robust deposition was obtained at Tris/PDMAEMA ratios of 2 and higher.

The dependency of PDMAEMA dissolution on the amount of Tris was causally related to the ensuing change in the solution pH as shown in Figure 1. This is likely because DMAEMA monomers are protonated at low pH and easily dissolvable in water due to intermolecular electrostatic repulsion. On the other hand, the monomers are deprotonated at high pH and may be difficult to dissolve in water because of intermolecular hydrophobic interactions. Indeed, Xiong et al. reported that the solubility of PDMAEMA-*b*-poly(acrylic acid) was altered by changing the pH of the solution.²²

We also observed that the interaction between PDMAEMA and pDNA was inhibited by increasing amounts of Tris (Figure 6). The inhibition was clearly observed at Tris/PDMAEMA weight ratios greater than 4:1 and was virtually complete at a ratio of 8:1. In addition, at the 8:1 ratio, the particle size of the polyplexes increased significantly (Figure 5), indicating the degradation of the polyplexes by weak interaction between PDMAEMA and pDNA. As mentioned above, PDMAEMA is protonated (cationic) at low pH (<7) and deprotonated at high pH (>8). Therefore, the loss of DNA binding was due to the disappearance of PDMAEMA ionic properties. The data from the electrophoretic gel shift assay and the above-mentioned thermoresponsive study led us to conclude that a Tris/PDMAEMA weight ratio of 2 is the optimal condition for transgene expression. Indeed, at this ratio, the significantly larger number of endocytosed Cy3-labeled plasmid DNA compared to that transfected using Tris-free PDMAEMA were observed in the primary ADCs (Figure 9B and C), and the highest level of transgene expression was obtained in HeLa cells, primary cardiac fibroblasts, and smooth muscle cells (Figure 6).

In general, transgene expression occurs after the release of pDNA from cationic polymers (decomplexation) in the cytosol or nucleus.¹² Therefore, the affinity between cationic polymers and pDNA inside the cells is a critical factor that determines efficient transfection. Indeed, Godbey et al. examined the effect of polyplex solution pH on the transfection efficiency by using poly(ethyleneimine) (PEI) as the transfection reagent.²³ However, this group found that the pH of PEI prior to forming a complex with pDNA did not create a significant difference from the transfection efficiency. This was because the pH adjustments made to the PEI/pDNA complex solutions were nullified once they were dipped into the culture medium. By contrast, in this study, we prepared the polyplex solutions at relatively high pH ranges from 8 to 11 by the addition of Tris (effective pH buffering range, 7–9) (Figure 1), and then coated the culture surface with them prior to adding cells suspended in media. In addition, the change in the affinity between PDMAEMA and pDNA that is due to altered solution pH was also observed when analyzed in electrophoresis buffer solution at a fixed pH of 8.3 (Figure 6). Therefore, the pH buffering of the polyplexes by Tris buffer could enhance their deposition in the culture surface microenvironment, after which they would be endocytosed by cells at a relatively higher pH when compared with the pH of the culture medium. This may contribute a more robust decomplexation of polyplexes during the endocytosis and cytosol trafficking inside cells.

After internalization of polyplexes, the first barrier for exit is considered to be endosomal escape. Indeed, it is well-known that the endosomal escape of polyplexes is a crucial rate-limiting step for efficient transfection. Here, polymers such as

PEI or PDMAEMA acquire a cationic charge due to protonation of their many amino residues at acidic pH (<7). When they are incorporated into endosomes, where the pH is relatively low (ca. 5–7), their cationic charges increased because of further protonation. This proton consumption causes destabilization and rupture of the endosome and ultimately leads to polyplex release via the so-called “proton sponge effect.”²⁴ Furthermore, Tris is known to bind DNA not only by electrostatic interactions, but also by hydrogen bonds.²⁵ Therefore, if polyplexes are combined with Tris through hydrogen bonds and endocytosed at relatively high pH, deprotonated PDMAEMA and Tris may consume a lot of protons in the endosome, further accelerating the proton sponge effect and associated polyplex release. In any case, further studies are required to delineate the mechanism by which Tris addition enhances the deposition transfection method.

In our previous study, we obtained sustained transgene expression for 2 weeks by deposition transfection using PDMAEMA.¹¹ Consistent with this, the enhanced luciferase expression by the addition of Tris at a Tris/PDMAEMA ratio of 2 was maintained for at least 10 days post-transfection in HeLa cells and also in primary cells (Figure 8). This suggests that the enhancement of transfection by the addition of Tris is continuous, rather than transient, and appears to occur without deleterious effects to the cells.

CONCLUSION

In this study, we increased the utility of deposition transfection technology by using Tris buffer as a pH adjuster for polyplexes solutions composed of PDMAEMA and pDNA. This leads to a dramatic enhancement of transfection efficiency in cell lines and in primary cells. We believe that our findings confirm that deposition transfection is a valuable method for many research and clinical fields, including regenerative medicine and gene therapy.

AUTHOR INFORMATION

Corresponding Author

*Tel: +81-6-6833-5012 (ex 2624). Fax: +81-6-6872-8090. E-mail address: nakayama@ri.ncvc.go.jp.

Notes

The authors declare no competing financial interest.

ACKNOWLEDGMENTS

The authors thank Mr. Shota Kusakabe for his technical assistance in this study. This work was supported in part by Grant-in-Aid for Young Scientists (Start-up, Grant Number 23860078) and Scientific Research (B23360374) from the Ministry of Education, Culture, Sports, Science and Technology of Japan and Intramural Research Fund for Cardiovascular Diseases (23-6-12) from the National Cerebral and Cardiovascular Center.

REFERENCES

- (1) Adler, A. F., and Leong, K. W. (2010) Emerging links between surface nanotechnology and endocytosis: impact on nonviral gene delivery. *Nano Today* 5, 553–569.
- (2) Zhang, S., Zhao, Y., Zhao, B., and Wang, B. (2010) Hybrids of nonviral vectors for gene delivery. *Bioconjugate Chem.* 21, 1003–1009.
- (3) Pandita, D., Santos, J. L., Rodrigues, J., Pêgo, A. P., Granja, P. L., and Tomás, H. (2011) Gene delivery into mesenchymal stem cells: a

biomimetic approach using RGD nanoclusters based on poly-(amidoamine) dendrimers. *Biomacromolecules* 12, 472–481.

(4) Santos, J. L., Pandita, D., Rodrigues, J., Pêgo, A. P., Granja, P. L., Balian, G., and Tomás, H. (2010) Receptor-mediated gene delivery using PAMAM dendrimers conjugated with peptides recognized by mesenchymal stem cells. *Mol. Pharmaceutics* 7, 763–774.

(5) Numata, K., Reagan, M. R., Goldstein, R. H., Rosenblatt, M., and Kaplan, D. L. (2011) Spider silk-based gene carriers for tumor cell-specific delivery. *Bioconjugate Chem.* 22, 1605–1610.

(6) Borchard, G. (2001) Chitosans for gene delivery. *Adv. Drug Delivery Rev.* 52, 145–150.

(7) Cheng, H., Zhu, J. L., Sun, Y. X., Cheng, S. X., Zhang, X. Z., and Zhuo, R. X. (2008) Novel thermoresponsive nonviral gene vector: P(NIPAAm-co-NDAPM)-b-PEI with adjustable gene transfection efficiency. *Bioconjugate Chem.* 19, 1368–1374.

(8) Zhou, Y. M., Ishikawa, A., Okahashi, R., Uchida, K., Nemoto, Y., Nakayama, M., and Nakayama, Y. (2007) Deposition transfection technology using a DNA complex with a thermoresponsive cationic star polymer. *J. Controlled Release* 123, 239–246.

(9) Chen, H., Zhang, H., Thor, D., Rahimian, R., and Guo, X. (2012) Novel pH-sensitive cationic lipids with linear ortho ester linkers for gene delivery. *Eur. J. Med. Chem.* 52, 159–172.

(10) Su, J., Chen, F., Cryns, V. L., and Messersmith, P. B. (2011) Catechol polymers for pH-responsive, targeted drug delivery to cancer cells. *J. Am. Chem. Soc.* 133, 11850–11853.

(11) Iwai, R., Kusakabe, S., Nemoto, Y., and Nakayama, Y. (2012) Deposition gene transfection using bioconjugates of DNA and thermoresponsive cationic homopolymer. *Bioconjugate Chem.* 23, 751–757.

(12) Wiethoff, C. M., and Middaugh, C. R. (2003) Barriers to nonviral gene delivery. *J. Pharm. Sci.* 92, 203–217.

(13) Kogure, K., Akita, H., and Harashima, H. (2009) Multifunctional envelope-type nano device for non-viral gene delivery: concept and application of Programmed Packaging. *J. Controlled Release* 122, 246–251.

(14) Miyata, K., Nishiyama, N., and Kataoka, K. (2012) Rational design of smart supramolecular assemblies for gene delivery: chemical challenges in the creation of artificial viruses. *Chem. Soc. Rev.* 41, 2562–2574.

(15) Troiber, C., and Wagner, E. (2011) Nucleic acid carriers based on precise polymer conjugates. *Bioconjugate Chem.* 22, 1737–1752.

(16) Kang, H. C., Samsonova, O., Kang, S. W., and Bae, Y. H. (2012) The effect of environmental pH on polymeric transfection efficiency. *Biomaterials* 33, 1651–1662.

(17) Lee, H., Son, S. H., Sharma, R., and Won, Y. Y. (2011) A discussion of the pH-dependent protonation behaviors of poly(2-(dimethylamino)ethyl methacrylate) (PDMAEMA) and poly(ethylenimine-ran-2-ethyl-2-oxazoline) (P(EI-r-EOz)). *J. Phys. Chem. B* 115, 844–860.

(18) Marfo, K., Garala, M., Kvetan, V., and Gasperino, J. J. (2009) Use of Tris-hydroxymethyl aminomethane in severe lactic acidosis due to highly active antiretroviral therapy: a case report. *Clin. Pharm. Ther.* 34, 119–123.

(19) Neethling, W. M., van den Heever, J. J., Cooper, S., and Meyer, J. M. (1993) Interstitial pH during myocardial preservation: assessment of five methods of myocardial preservation. *Ann. Thorac. Surg.* 55, 420–426.

(20) Franzblau, C., Pratt, C. A., Faris, B., Colannino, N. M., Offner, G. D., Mogayzel, P. J., Jr, and Troxler, R. F. (1989) Role of tropoelastin fragmentation in elastogenesis in rat smooth muscle cells. *J. Biol. Chem.* 264, 15115–15119.

(21) Nakayama, Y., Yamaoka, S., Nemoto, Y., Alexey, B., and Uchida, K. (2011) Thermoresponsive heparin bioconjugate as novel aqueous antithrombotic coating material. *Bioconjugate Chem.* 22, 193–199.

(22) Xiong, Z., Peng, B., Han, X., Peng, C., Liu, H., and Hu, Y. J. (2011) Dual-stimuli responsive behaviors of diblock polyampholyte PDMAEMA-b-PAA in aqueous solution. *J. Colloid Interface Sci.* 356, 557–565.

(23) Godbey, W. T., Wu, K. K., and Mikos, A. G. (1999) Size matters: molecular weight affects the efficiency of poly(ethylenimine) as a gene delivery vehicle. *J. Biomed. Mater. Res.* 45, 268–275.

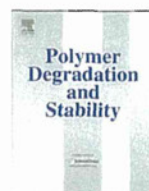
(24) Yang, S., and May, S. J. (2008) Release of cationic polymer-DNA complexes from the endosome: A theoretical investigation of the proton sponge hypothesis. *Chem. Phys.* 129, 18S105.

(25) Righetti, P. G., Magnusdottir, S., Gelfi, C., and Perduca, M. (2001) Behaviour of inorganic and organic cations in the Debye-Hückel layer of DNA. *J. Chromatogr., A* 920, 309–316.



ELSEVIER

Polymer Degradation and Stability

journal homepage: www.elsevier.com/locate/polydegstab

Polyethylene glycol-solvolyzed poly-(L)-lactic acids and their stereocomplexes with poly-(D)-lactic acid

Hisanori Ando^{a,*}, Maki Oshima^b, Yasuhide Nakayama^c, Atsuyoshi Nakayama^b^a Research Institute for Ubiquitous Energy Devices, National Institute of Advanced Industrial Science and Technology (AIST), 1-8-31 Midorigaoka, Ikeda, Osaka 563-8577, Japan^b Health Research Institute, AIST, 1-8-31 Midorigaoka, Ikeda, Osaka 563-8577, Japan^c Division of Medical Engineering and Materials, National Cerebral and Cardiovascular Center Research Institute, 5-7-1 Fujishiro-dai, Suita, Osaka 565-8565, Japan

ARTICLE INFO

Article history:

Received 9 October 2012

Received in revised form

18 February 2013

Accepted 25 February 2013

Available online 5 March 2013

Keywords:

Polylactic acid

Stereocomplex

Solvolytic

Polyethylene glycol

Contact angle

Biodegradation

ABSTRACT

Poly-(L)-lactic acid (PLLA) was solvolyzed with polyethylene glycol (PEG) with different ratios of PLLA and PEG under dry conditions. The obtained materials were found to be the block copolymer of PLLA and PEG (PLLA/PEG) from NMR analysis of which the number average molecular weights ranged from 6×10^3 to 2×10^4 g mol⁻¹. The films of stereocomplex (SC) of PLLA/PEG and poly-(D)-lactic acid (PDLA) were prepared by solvent casting method, and the thermal properties and the contact angle of the films were examined. The melting temperatures of PLLA/PEG and the corresponding SC with PDLA linearly decreased with the increase in the PEG content from 110 to 170 °C. The contact angle of PLLA/PEG became lower when the PEG content in the PLLA/PEG was higher, while their SCs with PDLA showed no clear correlation with the PEG content. Biodegradability of PLLA/PEGs and their SCs were also investigated with respect to the EG content.

© 2013 Elsevier Ltd. All rights reserved.

1. Introduction

The development of bioplastics, which can be produced from renewable resources, is one of the most important research topics in the “carbon neutral concept”, and thus varieties of research have been carried out so far [1]. Among the bioplastics, polylactic acid (PLA) is expected to be replaced with conventional thermoplastic polymers produced from petroleum resources because it shows excellent thermal and mechanical properties. However, it has some drawbacks, such as thermal stability, biodegradability and hydrophobicity, and these may be obstacles to the spreading of PLA.

Stereocomplex (SC) of PLA, firstly reported by Ikada et al., is a polymer blend obtained by mixing equimolar of poly-(L)-lactic acid (PLLA) and poly-(D)-lactic acid (PDLA) [2]. The SC has preferable properties compared with the homopolymers of PLA, such as high melting temperature, improved tensile strength, and high transparency [3–5]. Kimura et al. developed new block copolymers of PLLA and PDLA (stereoblock polylactic acids, sb-PLA), which effectively form SC with a molecular weight higher than 100 kDa [6].

We have previously synthesized L-lactide/glycidol copolymers at various compositions and reported that the thermal properties and biodegradability of the material are controllable simply by changing the comonomer feed ratio [7].

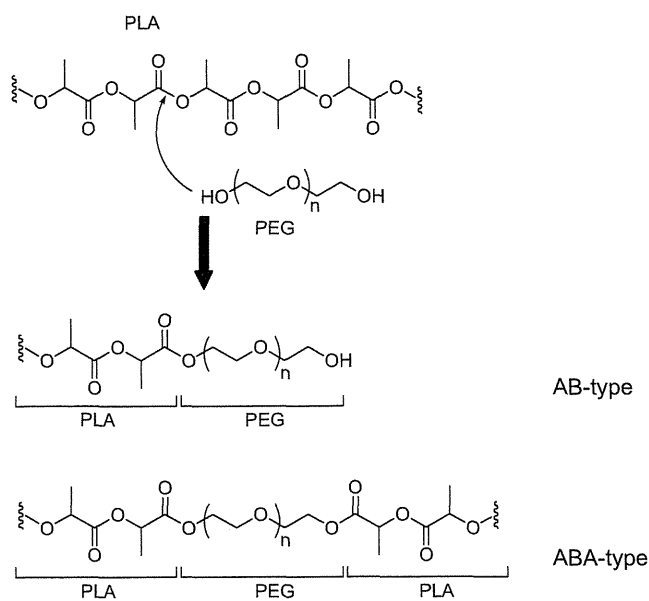
In the present study, we solvolyzed PLLA with PEG to produce the block copolymer of PLLA and PEG (PLLA/PEG) with various feed ratios and prepared its SC with PDLA to alter the hydrophilicity and biodegradability. Polyethylene glycol is a hydrophilic polymer having hydroxy groups at both ends which can react with the ester groups in PLA to give AB- and ABA-type block copolymers of PLA and PEG (see Scheme 1). The effects of PEG segment to the SCs on the thermal property, hydrophilicity and biodegradability are discussed on the basis of the results of the DSC, NMR, contact angle measurements and enzymatic hydrolysis using proteinase K.

2. Experimental

2.1. Materials

PLLA (Laclier[®], pellet) was supplied by Fuji Chemical. (D)-Lactide (PURASORB[®] D) and PEG with an average molar mass of 1000 were obtained from Purac Biochem and Sigma–Aldrich, respectively. Tetraphenyl tin (IV) and Proteinase K were purchased from Wako Pure Chemical Industries. All chemicals and solvents were of

* Corresponding author. Tel.: +81 72 751 9182; fax: +81 72 751 9629.
E-mail address: h-ando@aist.go.jp (H. Ando).



Scheme 1. Solvolysis of PLA with PEG.

special grade where obtainable and were used without further purification.

2.2. Synthesis of PDLA

(D)-Lactide (14.4 g, 100 mmol) was placed in a round-bottom flask (100 mL) equipped with a condenser and a desiccant tube. Tetraphenyl tin (IV) (0.13 g, 0.3 mmol) was added as solid, then the mixture was heated to 150 °C with stirring. The mixture became a pale yellowish solid after 8 h and the temperature was kept at 150 °C for 2 days. After cooling to room temperature, the solid was dissolved in a minimum volume of chloroform. The chloroform solution was poured into methanol with stirring, giving a fibrous precipitate. The precipitate was washed with methanol twice and dried at 50 °C under reduced pressure.

2.3. Solvolysis of PLLA

To avoid the hydrolysis of PLLA by residual water in the glass wares, they were subjected to a careful drying procedure under dried N₂ gas at 100 °C for several hours before use. PLLA and PEG were placed in a round-bottom flask (50 mL) equipped with a condenser and a desiccant tube and were heated at 100 °C with stirring under reduced pressure for 3 h to remove water. The reaction was initiated by raising the temperature to 220 °C. After 16 h, the reaction mixture was cooled down to room temperature, yielding the crude product (brownish hard solid). The crude product was dissolved in a minimum amount of chloroform, then the solution was poured into methanol with stirring to give precipitates. The precipitates were collected and washed with methanol twice, followed by vacuum drying.

2.4. Preparation of films

The polymer films were prepared by solvent casting method from the chloroform solution of the materials (3 w/v%) for several days, subsequently followed by vacuum drying at 50 °C. The films of SCs were prepared by using the mixture of the same volume of the chloroform solutions (6 w/v%) of PLLA/PEG and PDLA. All films were

dried at 50 °C under vacuum for several hours and stored in a desiccator.

2.5. Measurements

Gel permeation chromatography (GPC) was performed with HLC-8220GPC system (Tosoh, Japan) by using chloroform as eluant (0.6 mL min⁻¹) at 35 °C. Three columns, TSKgel 5000H_{xL}, TSKgel 4000H_{xL} and TSKgel 3000H_{xL} (Tosoh), were connected successively in this order. The number-average molecular weight (M_n) and the weight-average molecular weight (M_w) of the materials were calculated from the retention time of the polystyrene standard samples.

The thermal properties of the materials were investigated by differential scanning calorimetry (DSC), using a DSC3100S (Bruker AXS K.K., Japan). All the scans were carried out from 30 to 300 °C at a heating rate of 10 °C min⁻¹ under nitrogen atmosphere. Data for melting temperature (T_m) and the enthalpy of fusion (ΔH) were taken from the first heating scan.

¹H NMR spectra were recorded using a JNM-ECA-500 spectrometer (JEOL, Japan) (500 MHz for ¹H) at room temperature in CDCl₃ or D₂O with tetramethyl silane or sodium 3-(trimethylsilyl) propane-1-sulfonate as internal standards, respectively.

The static (equilibrium) contact angle of the films of PLLA/PEGs and their SCs with PDLA was measured with a Model-PGX (FIBRO System AB, Sweden) equipment. The samples for measuring the contact angle were deposited on the slide glass from 1 wt% chloroform solution of the material using simple spin coating at 3000 rpm for 35 s.

2.6. Enzymatic hydrolysis

The biological degradation of the materials was tested by the hydrolysis using Proteinase K in the 0.1 M phosphate buffer solution (NaH₂PO₄/Na₂HPO₄, pH = 7.0). The material (a piece of film, 20 mg) and the buffer solution of the enzyme (2 mL, 200 units) were placed in the test tube and heated at 37 °C for 48 h. After thermal denaturation of enzyme, the solution was filtrated with polytetrafluorethylene membrane (pore size, 0.2 μm) and water was removed in the drying oven at 60 °C. The deposited material was dissolved in D₂O for NMR analysis. The biodegradability was estimated from the integration of proton peaks of external standards of (L)-lactic acid and ethylene glycol. The data were corrected by subtracting both blank values; an enzyme blank level and a polymer blank level. The polymer blank level stands for standard nonenzymatic polymer hydrolyzability under the same conditions.

3. Results and discussion

3.1. PEG-solvolyzed PLLA

The properties of PLLA, PDLA and the PEG-solvolyzed PLLA (PLLA/PEG) are summarized in Table 1. The M_n values for the solvolyzed material ranged from 6.4×10^3 to 21×10^3 g mol⁻¹, depending on the PLLA/PEG feed ratio and reaction conditions. According to the M_w/M_n the solvolysis seems to proceed uniformly while the significant decrease of M_n and M_w was observed for all PLLA/PEGs compared with the original PLLA. The longer reaction time with higher temperature resulted in the product with extremely low M_n and M_w (runs 1 and 5).

As for ¹H NMR analysis, the peaks at δ 1.58 ppm (doublet) and δ 5.18 ppm (quartet) can be assigned to the methylene and methyl protons in $-\text{O}-\text{CH}(\text{CH}_3)-\text{C}(=\text{O})-$ fragment (LA) and δ 3.64 ppm (singlet) to the $-\text{O}-\text{CH}_2-\text{CH}_2-$ fragment (EG), where LA and EG represent the lactic acid unit and the ethylene glycol unit, as diad homo sequences ($-\text{LA}-\text{LA}-$, $-\text{EG}-\text{EG}-$), respectively. The weak

Table 1
Properties of PEG-solvolyzed PLLA under various reaction conditions.

Polymerization conditions					Physical/chemical properties of the materials								
Run	PLLA g(mmol)	PEG g (mmol)	Temp. (°C)	Time (h)	M_n ($\times 10^{-3}$)	M_w ($\times 10^{-3}$)	M_w/M_n	T_m (°C)	ΔH (kJ g^{-1})	EG cont. (%) ^a	Copolymer cont. (%) ^b	[EG _{est.} cont.] (%) ^c	[EG _{Theor.} cont.] (%) ^d
L	PLLA	—	—	—	92	127	1.4	162	43	—	—	—	—
D	PDLA	—	—	—	44	64	1.5	176	51	—	—	—	—
1	5 (0.05)	0.5 (0.5)	190	12	21	34	1.7	164	39	4.9	65	7.5	14
2	5 (0.05)	0.25 (0.25)	190	12	18	34	1.8	157	41	3.8	43	8.8	7.6
3	5 (0.05)	0.1 (0.1)	190	12	21	35	1.7	158	45	0.67	9	7.6	3.2
4	5 (0.05)	0.05 (0.05)	190	12	12	17	1.5	161	43	0.22	2	13	1.6
5	5 (0.05)	0.5 (0.5)	220	18	6.4	7.8	1.2	126	30	6.5	28	23	14
6	5 (0.05)	0.005 (0.005)	220	18	8.9	11	1.3	108	11	17	99	17	0.16

^a Calculated from the peak intensity of ¹H NMR spectrum. The details are described in the text.

^b Calculated from the ratio of EG cont. and EG_{est.} cont.

^c Calculated from the GPC result. The details are described in the text.

^d Calculated from the feed ratio of PLLA and PEG.

peaks at $\delta 4.32$ – 4.22 ppm and $\delta 3.75$ – 3.67 ppm were also observed which can be assigned to the methylene protons in the hetero connecting fragment ($-\text{LA}-\text{EG}-$) and $\delta 4.36$ ppm (quartet) can be assigned as a methyne proton in an end group of LA. Observation of the hetero sequence means that the block copolymer is successfully produced (see Fig. 1). A block length of the PEG segment in run 1 was calculated from the intensity ratio of the protons of homo and hetero sequences. The value is ca. 25. The molecular weight of the repeating unit of PEG segment is 44, meaning that the molecular weight of PEG segment in the copolymer is ca. 1100. This is almost the same as the original molecular weight of PEG. The results show that a PLLA/PEG molecule contains one PEG segment in both AB-type and ABA-type block copolymers. The EG content (%) in PLLA/PEG was calculated from the peak intensity (I) according to equation (1), as the ¹H NMR signals from the terminal protons of PLLA and PEG are negligibly small compared with those from the main body.

$$\text{Obsd. EG cont. (\%)} = \frac{I_{[\delta 3.64]}}{(I_{[\delta 1.58]} + I_{[\delta 3.64]} + I_{[\delta 3.64]})} \times 100 \quad (1)$$

The EG content was also estimated from the M_n obtained by GPC. The molecular weight of repeating unit of PLLA ($-\text{OCH}(\text{CH}_3)\text{CO}-$) and PEG ($-\text{O}-\text{CH}_2-\text{CH}_2-$) are 72 and 44, respectively, then the EG content can be calculated by the following equation:

$$\text{GPC Est. EG cont. (\%)} = \frac{U_{\text{EG}}}{(U_{\text{LA}} + U_{\text{EG}})} \times 100 \quad (2)$$

where U_{EG} and U_{LA} are the number of the repeating units for EG and LA, respectively, and they can be calculated by the equations as follows when the molecular weight of PEG is 1000:

$$U_{\text{EG}} = 1000/44 = 22.7$$

$$U_{\text{LA}} = (M_n - 1000)/72$$

In comparison with the estimated EG content from GPC results, some observed EG contents are small. For example, the observed EG content (3.8%) was significantly low compared with that from GPC (8.8%, run 2). That is, LA content in the obtained polymer is larger than the estimated value from GPC, suggesting that the obtained

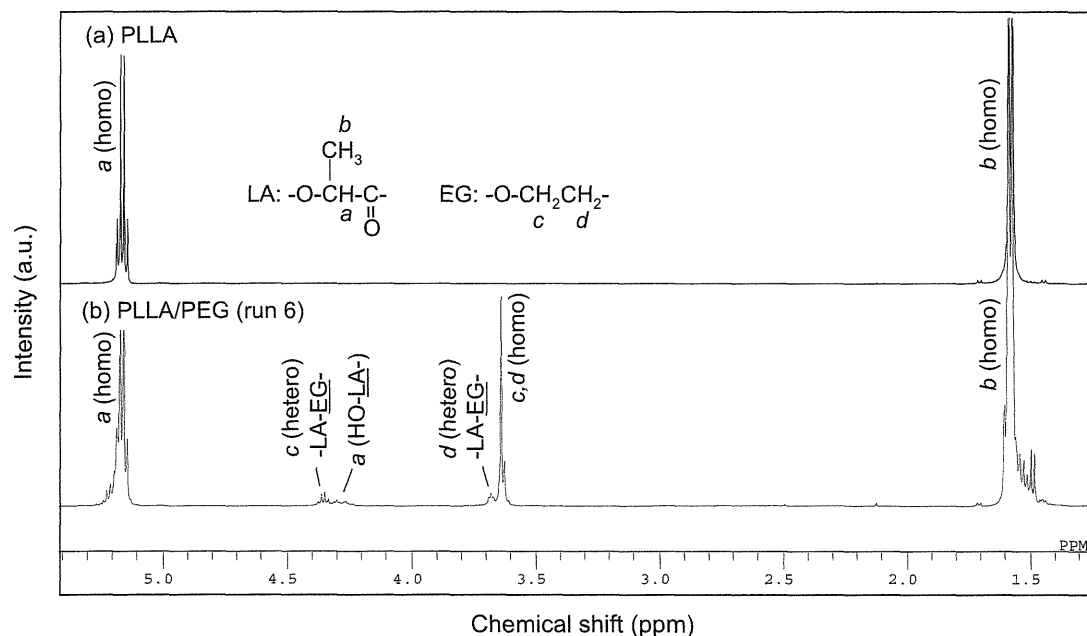


Fig. 1. ¹H NMR spectra of PLLA (a) and PLLA/PEG (run 6) (b).

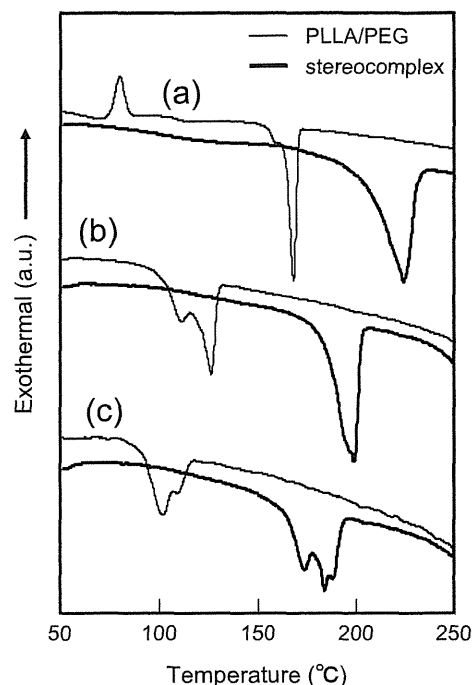


Fig. 2. DSC profiles of the PLLA/PEGs (drawn with lines with normal thickness) and SCs with PDLA (with bold lines): (a) PLLA (run L), (b); run 5, (c): run 6.

polymers contain the unreacted PLLA homopolymers. Copolymer content in the mixture of copolymers and PLLA homopolymers are calculated from the difference between EG content and the estimated one. From runs 1 to 4, the copolymer contents decreased with the decrease in feed PEG ratio because of a low reaction rate with a small amount of reactant. In cases of runs 5 and 6, copolymer contents are high because of a high reaction temperature.

Since PEG is soluble in methanol, low molecular weight block copolymers were removed during the purification process, then most of the observed EG content were smaller than those of theoretical EG content which was calculated from the feed ratio of PLLA and PEG. As for run 6, the EG content is larger than that of theoretical EG content. It is reasonable to say that the removal of lactide took place because of the pyrolysis of PLLA by high reaction temperature.

3.2. Thermal properties

In Table 1, the PLLA used was purchased one and small amount of D-lactide unit was contained. Therefore, T_m was slightly low and ΔH was small compared with those of PDLA which was prepared by the polymerization of D-lactide with high optical purity. The copolymers in runs 3 and 4 showed high ΔH s because of their high LA content. Fig. 2 shows the DSC profiles of PLLA, PLLA/PEGs (runs 5 and 6) and their SCs with PDLA. The melting temperature (T_m) of

Table 2
Thermal properties of SCs of PLLA/PEGs with PDLA.

Run	T_m (°C)	ΔT_m (°C)	ΔH (kJ g ⁻¹)
L	225	57	63
1	225	61	67
2	223	66	65
3	226	68	54
4	225	64	66
5	199	73	52
6	184	76	33

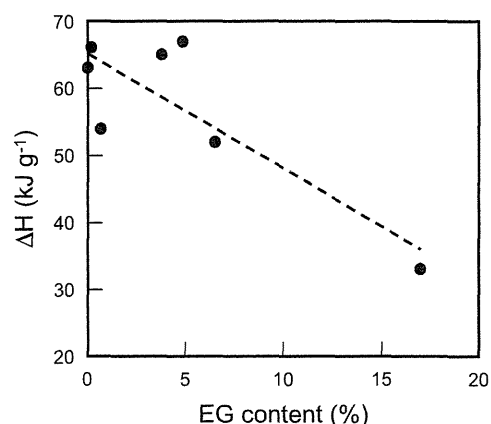


Fig. 3. Enthalpies of fusion of SC vs EG content in PLLA/PEG.

PLLA/PEGs became lower with the decrease in the molecular weight and LA content. In the comparison with runs 5 and 6, the copolymer in run 5 showed higher T_m in spite of the lower molecular weight because of the higher LA content. When PLLA/PEG and PDLA were mixed, the material melted at significantly higher temperatures than each component, suggesting that these two components interact with each other to form SCs. The ΔH values of SCs were always larger than those of the PLLA/PEGs (see Table 2), meaning that the materials became thermally more stable by forming SCs. Fig. 3 shows the relationship between the EG content in PLLA/PEG and ΔH of the SCs with PDLA. It is clearly seen that the value of ΔH decreases with the increase in the EG content. This means that the EG segment suppresses the crystallinity of SC.

When the T_m of the SC is plotted against that of the corresponding PLLA/PEG, a linear relationship was observed with a high correlation coefficient (see Fig. 4). This information enables us to estimate the T_m of the SC from the corresponding PLLA/PEG, and then is useful for the molding process in the polymer industry. The similar tendency was reported for the L-lactide/ ϵ -caprolactone random copolymer and their SCs with PDLA [8].

3.3. Surface hydrophilicity

The surface hydrophilicity of the PLLA/PEGs and their SCs were estimated by measuring the contact angle. As seen in Fig. 5 the

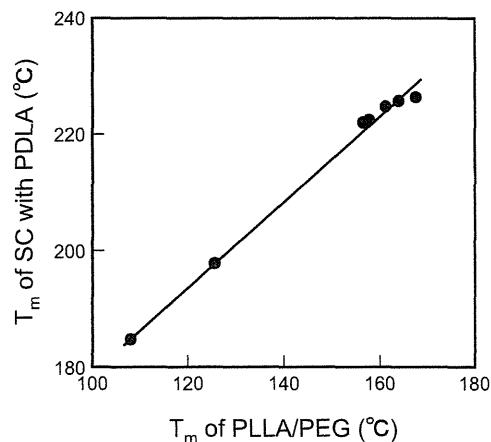


Fig. 4. Relationship between the melting temperatures of the PLLA/PEGs and their SCs with PDLA.

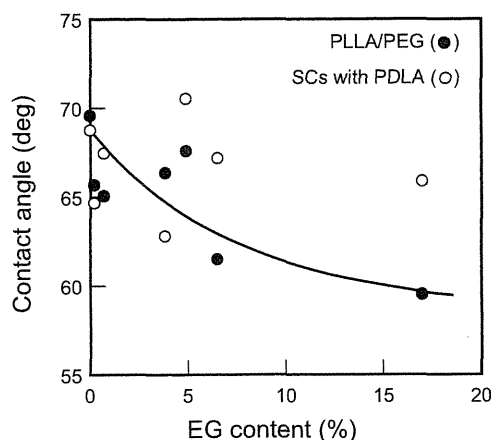


Fig. 5. Contact angle vs EG content of PLLA/PEGs and their SCs with PDLA: (●), PLLA/PEG; (○), SC with PDLA.

contact angle significantly decreased with the increase in the EG content of PLLA/PEG (●), showing that the hydrophilicity of PLLA increased by incorporating the EG fragment into the PLLA structure. On the other hand, the contact angle of the SCs with PDLA gave no clear correlation with the PEG content (○). This can be explained that the hydrophilic segment in the structure may be buried or turned into inside when the SC is formed in the chloroform solution, and then the hydrophobic part was arranged outside during the SC formation process, while the detail of the effect of EG fragment on the hydrophilicity is still unclear.

3.4. Biodegradability

PLLA is degradable under the natural environmental conditions, while the SC of PLLA and PDLA is known to have low biodegradability and high hydrolysis-resistance. In order to investigate the contribution of the PEG fragment in the PLLA/PEGs to the degradability, the enzymatic hydrolysis of the SCs of PLLA/PEGs with PDLA was carried out using Proteinase K in the phosphate buffer solution.

Fig. 6 shows the plots of the degradation (left Y-axis) and the residual weight (right Y-axis) vs. EG content. There are two types of SCs formed with PLLA/PEG and PLLA homopolymers. The SC mixtures seem to be morphologically homogenous because all the data were on the same biodegradation curve. The degradation of the SCs proceeds more with the increase in the EG content of PLLA/PEG, resulting in more water-soluble products and consequently leaving less residues. On the basis of NMR analysis, a variety of compounds was found in the degradation product, including lactic acid and oligo-lactic acids, some of which were assigned to PEG-adducts.

The enzymatic hydrolysis proceeded on the SCs by incorporating the PEG fragment into PLLA. Since the high crystallinity of SCs is thought to be the main reason for the low degradability, the PEG fragment might reduce the crystallinity as described above (cf. Fig. 3). The frayed space or spatial gap induced by the mismatch

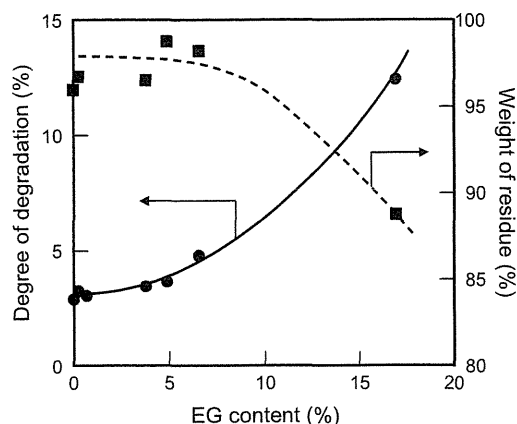


Fig. 6. Biodegradability vs. EG content of the SCs prepared from PLLA/PEG and PDLA.

between PEG fragment and PDLA may give a chance to attack the main chain of lactic acid.

4. Conclusions

A block copolymer of PLLA and PEG was successfully prepared by solvolysis without catalyst. On the basis of the GPC and NMR analyzes the M_n and EG content of the PLLA/PEGs were lower than those expected. The melting temperatures of PLLA/PEGs and their SCs with PDLA showed a linear relationship which enables us to estimate the melting temperature of the SC of PLLA/PEG copolymer and PDLA. The surface hydrophilicity increased with the increase in the EG content of the PLLA/PEGs while no clear dependency of the hydrophilicity on the PEG content was observed in their SCs with PDLA. The incorporating of PEG to PLLA accelerated the enzymatic hydrolysis of the SCs. These findings may lead to the development of a new type of hydrophilic and biodegradable polymer materials based on polylactic acid.

References

- [1] Luckachan GE, Pillai CKS. Biodegradable polymers – a review on recent trends and emerging perspectives. *J Polym Environ* 2011;19(3):637–76.
- [2] Ikada Y, Jamshidi K, Tsuji H, Hyon SH. Stereocomplex formation between enantiomeric poly(lactides). *Macromolecules* 1987;20(4):904–6.
- [3] Chang L, Woo EM. A unique meta-form structure in the stereocomplex of poly(D-lactic acid) with low-molecular-weight poly(L-lactic acid). *Macromol Chem Phys* 2011;212(2):125–33.
- [4] Tsuji H, Yamamoto S. Enhanced stereocomplex crystallization of biodegradable enantiomeric poly(lactic acid)s by repeated casting. *Macromol Mater Eng* 2011;296(7):583–9.
- [5] Nouailhas H, Li F, Ghzaoui AE, Li S, Coudane J. Influence of racemization on stereocomplex-induced gelation of water-soluble poly(lactide)-poly(ethylene glycol) block copolymers. *Polym Int* 2010;59(8):1077–83.
- [6] Kakuta M, Hirata M, Kimura Y. Stereoblock poly(lactides) as high-performance bio-based polymers. *J Macromol Sci Part C: Polym Rev* 2009;49(2):107–40.
- [7] Petchsuk A, Nakayama A, Aiba S. Synthesis and biodegradability of L-lactide/glycidol copolymers. *Polym Degrad Stab* 2009;94(10):1700–6.
- [8] Nakayama A, Kawasaki N, Yamamoto N, Aiba S. In: . Proceedings 10th Pacific polymer conference 2007;vol. 6. p. 168.

体内で作るバイオマテリアル (生体内バイオマテリアル)

中山 泰 秀*

1. はじめに

日本語で「生体材料」または「医用材料」と呼ばれる「バイオマテリアル」は、生体成分と接触する診断機器から体内埋め込み型の人工臓器などの治療機器まで、薬事法上「医療機器」に含まれるものの材料として臨床において広く用いられている。その素材の多くは、「金属」や「セラミックス」、「高分子」などの汎用性工業製品からなる人工物であり、一部タンパク質や多糖などの天然物も含まれるが、それらのほぼ全ては患者自身の体内にはもともと存在していなかった異物である。従って、バイオマテリアルの安全性を保証するために、可滅菌性、非毒性、機能性、生体適合性、耐久性などの必要条件を満たすことが要求される。

一方、患者自身の組織を用いて治療が行われている例として、虚血性心疾患に対する手術的治療

法である冠動脈バイパス移植術がある。狭窄した冠動脈の遠位側に大動脈または内胸動脈等から血管をつなぎ、狭窄部をバイパスすることで血流量の回復をはかる手術である。バイパス用血管として患者自身の静脈や動脈が、ある種バイオマテリアルとして用いられている。必要な血管の径は3 mm 以下と細いために、人工材料では血栓や内膜肥厚などで閉塞しやすい。そのため、長年にわたる多大なるバイオマテリアル研究にも関わらず、満足できる開存性を維持できるバイパス用の小口径人工血管は開発されておらず、最もハードルの高い人工臓器の一つとなっている。従って、移植用の人工臓器・組織に用いられるバイオマテリアルの究極の目標は、患者自身の臓器や組織つまり自家移植体であるともいえる。

そこで自己の組織を再現しようと登場したのが、生体外での組織工学(in vitro tissue engineering)に基づく再生医療技術である。それを用いた移植用組織体の一般的な作製方法を図1に示す。まず患者自身の組織や細胞が採取され、組織処理によ

* Yasuhide Nakayama 独立行政法人国立循環器病研究センター研究所 医工学材料研究室 室長 工学博士
Completely Autologous Biomaterials Prepared by In Body Tissue Architecture Technology

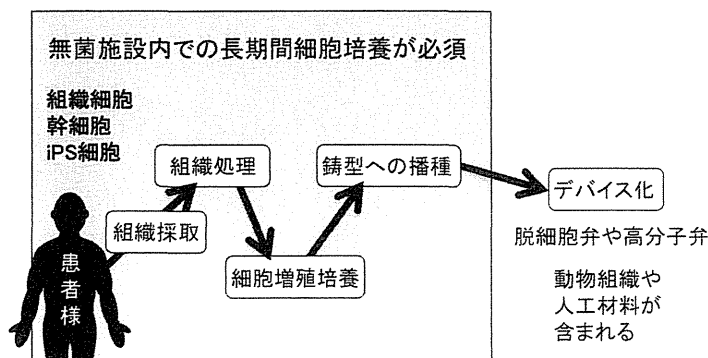


図1 従来の生体外組織工学に基づく再生医療技術による移植用組織体の作製方法(心臓代用弁の例)

て分離・精製された後、培養によって大量に細胞が増殖され、それが高分子製や動物組織からなる鋳型に播種され、必要に応じて力学的負荷をかけながら再培養によって生着させることで、通常数ヵ月の期間を要してデバイスとして移植用の組織体を得られている。一般に再生医療における三要素と呼ばれる、細胞、その接着の足場となるスキャホールド材と細胞成長因子を含む培養条件が組み合わされている。既に血管組織体や皮膚組織体などがベンチャー企業によって商品化されている。しかし、特別な高度滅菌施設において煩雑な細胞操作を繰り返す必要があり、生分解性材料を用いた一時的な場合もあるがスキャホールド材となる人工材料が含まれ、少なくとも培養液成分が残るため、得られる組織体は完全な自己組織体とはいえない。

われわれの研究グループでは、体内に一時的に高分子製の鋳型を埋入することで、その周囲に形成される新生自己組織をバイオマテリアルと見立て、得られる生体内バイオマテリアルを用いて移植用の組織体を作製する技術を「生体内組織形成術 (in body tissue architecture technology)」と名付けて開発を進めてきた。図2に示すように、培養操作や滅菌施設を一切必要とせず、単に鋳型を皮下に入れておくだけで、ほぼ自動的に確実に正に究極のバイオマテリアルが簡単にできあがる。従って、本技術で得られる生体内バイオマテリアルには多くの利点がある。例えば、鋳型の埋入数や形によって、①多量に得られ、②形状を自由に

設計できる。さらに自己組織のみで構成されるため、③免疫反応がなく、④毒性がなく生体適合性に優れており、⑤感染症において有利と考えられる。また、⑥移植後に体内で成長できる可能性も期待される。

本稿では、まず生体内組織形成術の原理と得られる生体内バイオマテリアルの性質について説明し、次いで生体内バイオマテリアルの形成促進化や機能化のための基盤技術の開発状況について、最後に主に循環系移植医療に取り組んでいる中でバイオチューブやバイオペルブと名付けた代用血管や心臓代用弁への応用例を紹介する。

2. 生体内バイオマテリアルについて

皮下に人工物などの異物を埋入すると、生物学的に不活性で毒性が無ければ、人工物を皮下の結合組織が取り囲むカプセル化(被包化)が異物反応の一種として起こる。このカプセル組織体が生体内バイオマテリアルとなる。カプセル組織体は主として皮下組織から移動した、あるいは脂肪内に存在する幹細胞から一部分化した線維芽細胞によって形成される。数週間から数ヵ月間で人工物の周囲はほぼ完全に高密度のコラーゲン膜で覆い尽くされ、カプセル化は完了する。このカプセル化反応は、多くの埋め込みを伴う外科手術で日常的に経験される。例えば、皮下に埋入されたペースメーカーの電池交換の際などにも、周囲に形成された硬いコラーゲン膜を切開して内部の電池が取出されている。

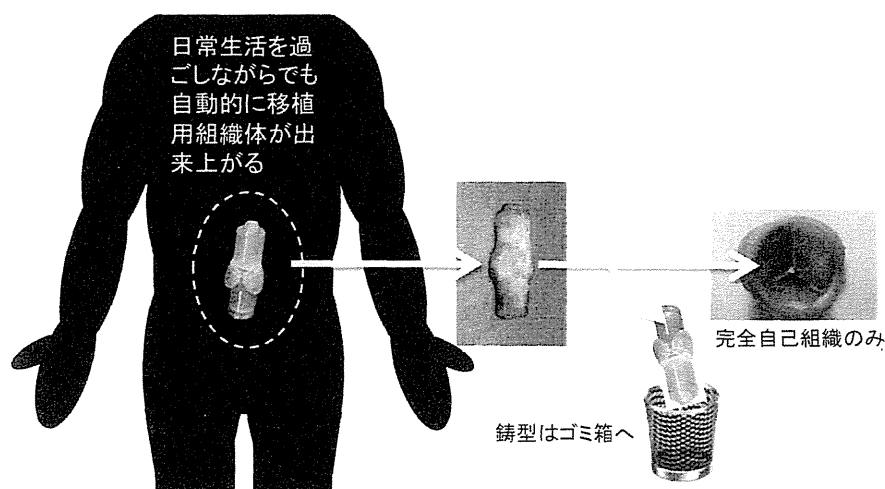


図2 生体内組織形成術による新発想の再生医療技術に基づく自家移植用組織体の作製方法(心臓代用弁の例)

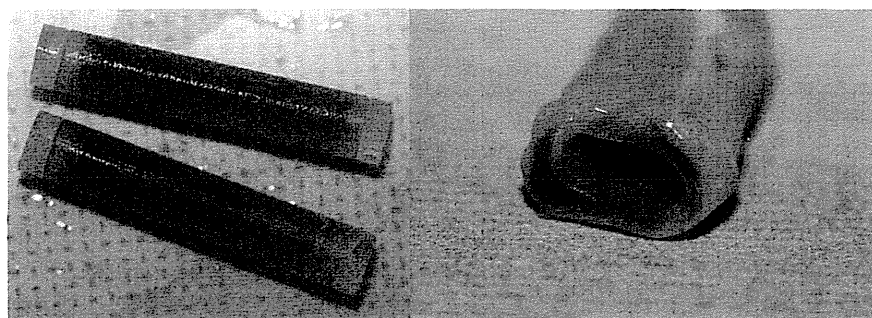


図3 色素徐放型鋳型(左)とその鋳型を用いて2週間後に得られた高膜厚バイオチューブ人工血管(右)

医療機器の材料として用いられているシリコン、アクリル、ポリウレタン、ポリ塩化ビニル、ポリエチレン、ポリスチレン、テフロンなどの汎用性高分子樹脂を動物皮下に埋入すると、数週間後には全ての埋入物の周囲は薄い膜状のカプセル組織体で覆われる¹⁾。従って、基本的にこれらの樹脂は全て生体内バイオマテリアル作製の鋳型の材料として用いることができる。細胞実験ではテフロンなどの高撥水性表面やハイドロゲルのような高含水性表面では細胞接着がほとんど起こらず、細胞死に至るが、生体内においては、それらの表面物性を有する材料においてもカプセル化はほぼ全てで起こる。

生体内バイオマテリアルはカプセル化によって得られるため、その細胞成分は必然的に線維芽細胞が主となり、一部筋線維芽細胞や血管新生に伴う内皮細胞や平滑筋細胞も存在している¹⁾。好中球やマクロファージといった炎症性細胞はほとんど含まれない。一方、細胞外マトリックス成分は、ほぼ網目状のI型コラーゲン線維である。しかし、最近の研究ではエラスチンや、移植対象にあった細胞種を存在させることも可能となっている。また、カプセル組織体の形成性は、埋入基材の弾性率や膨潤性、形状などの物理的性質、分子組成などの化学的性質、生理活性などの生物学的性質など多くのパラメーターに大きく依存する。そのため、単純に汎用性高分子の中から基材を選択するだけでも、生体動脈の中の比較的強固な冠動脈から柔軟な頸動脈まで力学性質を異にする生体内バイオマテリアルの作り分けが可能である¹⁾。

3. 生体内バイオマテリアルの作製促進技術

生体内バイオマテリアルの形成は、VEGFやbFGFなどの細胞増殖因子を直接あるいはゲル内に包埋して鋳型表面に塗布することで、結合組織の形成を早め、さらに新生血管を積極的に誘導できる。また、血管新生作用のあるニコチンを用いても同様な効果が得られている²⁾。最近では、特別な薬理活性の知られていない食用色素などを徐放化させることでマテリアル形成が一層促進され、週単位でのカプセル組織体の作製が可能であることも見出された(図3)³⁾。不活性な有機化合物を用いても生体反応を間接的に惹起させることができ、薬剤と同等以上に組織形成を促進させる効果が得られた。また、鋳型の表面微細形状によっても生体反応を刺激でき、促進効果が観察されている。ミクロンレベルの凹凸パターンを鋳型表面の一面に作製すると、同じ埋入期間において、強度が高く、壁の厚い組織を有するバイオマテリアルが形成されている(図4)。

さらに、生体反応を能動的に促進させる手段として、体内における光照射の影響が調べられている⁴⁾。青色LEDを初期の2日間照射することで、3週間後には通常得られる管状バイオマテリアルの約5倍の厚さが形成され、さらに得られたバイオマテリアル内にエラスチン線維の産生も起った。弁や血管の構成成分を光照射によって予め準備しておくことで、マテリアルを移植した後の再生が加速されると期待される。

4. 生体内バイオマテリアルの人工血管(バイオチューブ)への応用

大血管に対する人工血管の完成度はかなり高いといえるが、内径6mm未満の小口径人工血管については血栓形成や内膜肥厚の問題から実用化ま

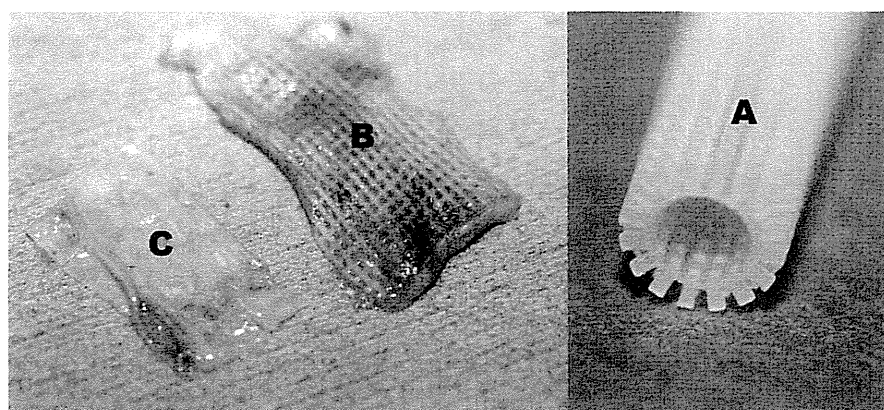


図4 表面にマイクロレベルの突起を有する凹凸铸型(A)とその铸型を用いて得られた生体内バイオマテリアル(B)、従来のシリコン円柱を铸型としてこれまで得られていた生体内バイオマテリアル(C)

ではいたっておらず、先述したように冠動脈や下肢末梢動脈へのバイパス術には内胸動脈や大伏在静脈といった自己の血管がグラフトとして用いられている。それゆえバイパス手術の再手術が必要な場合や下肢静脈瘤などで血管の性状が良好でない場合、下肢切断後などの場合には使用できるグラフトが制限されるという問題がある。そこで、生体内組織形成技術によって得られた管状の生体内バイオマテリアルをバイオチューブ人工血管として、小口径代替血管への応用を検討している^{5~7)}。

シリコン製铸型をそれぞれビーグル、ウサギ、ラット皮下に埋入した。4週後に摘出し、カプセル化された状態で摘出した後、内部の铸型を抜去することで、管状の結合組織体であるバイオ

チューブを得た。それぞれビーグル総頸動脈(内径：4~6 mm)、ウサギ総頸動脈(内径：2~3 mm)、ラット腹部大動脈(内径：1.5~2 mm)に移植した(図5)。バイオチューブの表面はコラーゲンや線維芽細胞が露出しているため血栓性である。しかし、アルガトロバンなどで予め抗血栓性処理を施しておくことで開存率を大幅に向上することができた⁸⁾。術後は抗血小板剤や抗凝固剤を投与することなく、現在も経過観察中ではあるが最長でビーグルでは約4年、ウサギでは約2年、ラットでは約半年の長期開存が得られており瘤化や狭窄は認めていない。また、グラフト摘出後の組織学的評価では約2週間で完全な内皮化が起こり、さらに植込み後約12週で壁内の細胞は平滑筋細胞に置き換わり、エラスチンの発生も認められ、

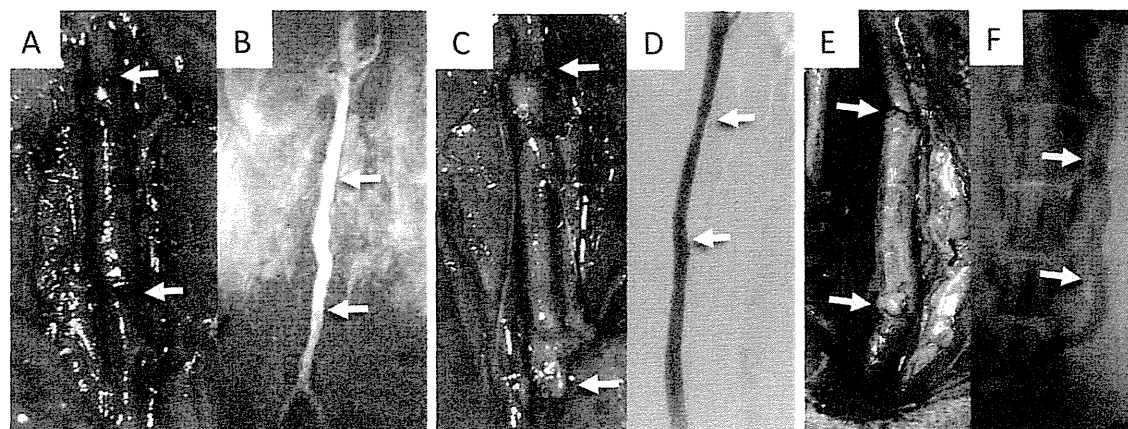


図5 バイオチューブ人工血管の移植例。内径1.5 mm, 2 mm, 5 mm のバイオチューブ人工血管を、それぞれラット腹部大動脈(A)、ウサギ総頸動脈(C)、ビーグル総頸動脈(E)に移植した(吻合部を矢印で示す)。ラット移植3ヵ月後のMRA像(B)、ウサギ移植6ヵ月後(D)、ビーグル移植1年後(F)の血管造影像による開存性の確認

生体血管と肉眼的に見分けがつかない程に成熟していた⁶⁾。バイオチューブは、僅かに移植時の抗血栓性処理を施すだけで、移植後早期に血管組織へと置き換わる、生体適合性に優れ、高い再生能を有するバイオマテリアルといえる。

5. 生体内バイオマテリアルの心臓人工弁(バイオバルブ)への応用

重度の弁膜症に対する弁置換術に用いられている人工弁には機械弁、生体弁があるが、機械弁における抗凝固療法の必要性や生体弁の低い耐久性といった問題がある。また、小児への移植においては成長の問題もある。これらの問題に対し、以前より自己細胞による組織工学が注目され、最近では生分解性ポリマーに自家細胞播種を組み合わせたハイブリッド型の心臓代用弁が開発され、特に小児において右心系などの低圧系で臨床応用が進められ良好な成績が収められている。しかしこれらの弁においても左心系などの高圧系での応用は破裂や瘤化のため困難とされる。

われわれは、生体に4つある心臓弁のうちバルサルバ洞(肺動脈弁では肺動脈洞)と呼ばれる3つの膨らみと、それぞれの内部に半月状の弁葉を有する三葉弁形状の大動脈弁と肺動脈弁の開発に取り組んでいる^{9~11)}。その3次元構造体を作製するために、2種類の凹凸型のアクリル製の円柱基材を組み合わせて鋳型とし、弁葉形成部となる隙間を凸型基材の外周部に設けるように設計した(図6)。凹型には洞形状に似せた3つの膨らみを付け、凸型はほぼ円柱とした。これを1ヵ月間ビー

グル犬やヤギの皮下に埋入させた。凸型基材の内部にカプセル内視鏡を内蔵させて、体内での弁葉の形成過程を非侵襲で経時的に観察することで、完了時期を確認後に鋳型を摘出した¹²⁾。バイオチューブの場合と同様に内部の鋳型を抜き取ると、従来同様にコラーゲンと線維芽細胞を主体とする生体内バイオマテリアルからなり、内腔面に三葉弁が開口位で強固に一体化したバイオバルブ人工弁が得られた。補助人工心臓用耐久試験装置(ラボハート NCVC)を用いた拍動回路実験において、大動脈弁に相当する環境下で1ヵ月以上逆流率15%以下が維持されたことから、生体内バイオマテリアルは極めて耐久性に優れ、またバイオバルブは機能性に優れていることが実証された。

動脈圧負荷に対する慢性的な耐久性を評価する目的で、左心系バイパス(Apico-Aortic bypass)術を用いて、バイオバルブを人工血管の途中に挟み

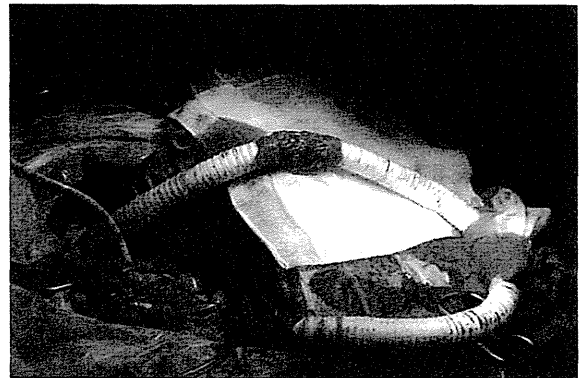


図7 バイオバルブ人工弁の移植例。心臓心尖部から下行大動脈へのバイパス(Apico-Aortic bypass)途中にバイオバルブ人工弁を移植して耐久性を評価している

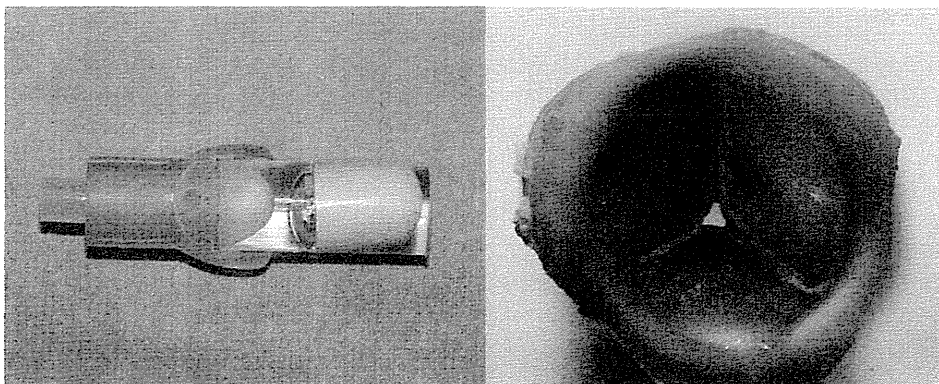


図6 バイオバルブ心臓弁作製用のカプセル内視鏡内蔵型鋳型(左)とその鋳型を用いて得られたバイオバルブの末梢側からの3葉弁葉の観察(右)

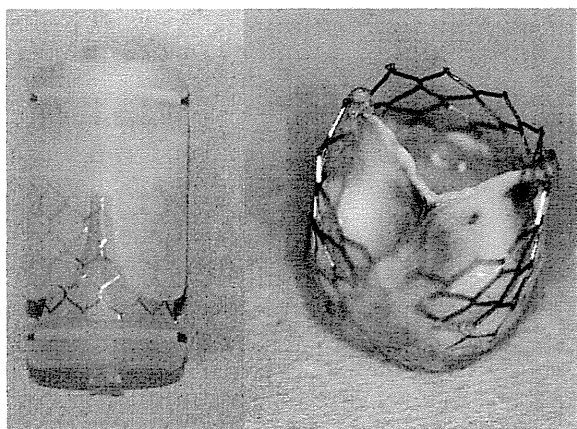


図8 経カテーテル的大動脈弁植え込み術が可能なステント型バイオバルブ(右)とその作製用鋳型(左)

込むようにヤギへの移植実験を行った(図7)¹³⁾。術後、動脈圧 100~150 mmHg, 血流量 2.5~4 L/min を維持した。血管造影および経胸壁エコーにてバイパスグラフトの血流は良好で、弁葉の可動性も良く、顕著な狭窄や逆流もなく経過した。術後2ヵ月に摘出すると内腔面に血栓はほとんどなかった。導管部は元のバイオバルブ組織が α -SMA 陽性細胞を含む血管壁を構成する組織体へと変わった。弁葉組織内では導管部と同様に豊富な血管新生が起こり、さらに弁尖へ向かって浸潤する多数の α -SMA 陽性細胞を認めた。バイオバルブ組織内に移動した周囲細胞が血管壁構成細胞に分化し、再生へと導いていると考えられた。バイオバルブは血管と接合されていない極めて不利な条件下においても優れた再生能力を発揮した。自己組織のみからなる組織工学弁の大動脈弁への応用は世界初である。

最近では、低侵襲で弁置換ができる、経カテーテル的大動脈弁植え込み術(Transcatheter Aortic Valve Implantation: TAVI)用として、ステントとバイオバルブが一体化したステント付バイオバルブを開発し、ヤギやビーグル犬への移植実験を進め、臨床応用をめざしている(図8)¹⁴⁾。

6. おわりに

生体内組織形成技術を用いることで、煩雑な細胞培養などを必要とせず、より簡便、安全にそして低コストで自己組織のみからなる生体内バイオマテリアルで自家移植用組織を作製することがで

きる。生体内バイオマテリアルは、免疫性、感染において有利であり、将来の成長性が期待できる。現在、バイオチューブ人工血管、バイオバルブ人工弁それぞれ移植後の耐久性や組織学的変化などを長期で観察を行っている。通常のバイオマテリアルと異なり、移植期間が長くなればなる程、生着によって移植対象組織体へと再生が進む。生体内組織形成術では、わずか数週間で移植に耐える生体内バイオマテリアルからなる組織体をいとも簡単に作製する。それは現在の最新の技術と設備を駆使しても人工的には不可能である。今後生体内組織形成術を用いた新たな再生医療が実際の一般治療として普及することが大いに期待される。

謝辞

本研究は、京都府立医科大学心臓血管外科の神田圭一講師のグループ、日本大学獣医学科の上地正実教授のグループ、関西大学流体工学・バイオメカニクス研究室の大場謙吉名誉教授、田地川勉講師のグループ、国立循環器病研究センター研究所人工臓器部の巽英介部長、武輪能明室長のグループと共同で行ってまいりました。ここに深謝申し上げます。また、研究に熱意を持って取り組んでくれた医工学材料研究室の皆様感謝いたします。

参考文献

- 1) Nakayama Y, Ishibashi-Ueda H, Takamizawa K: In vivo tissue-engineered small-caliber arterial graft prosthesis consisting of autologous tissue (biotube). *Cell Trans* 13: 439-449, 2004.
- 2) Sakai O, Kanda K, Takamizawa K, Sato T, Yaku H, Nakayama Y: Faster and stronger vascular "Biotube" graft fabrication in vivo using a novel nicotin-containing mold. *J Biomed Mater Res B* 83B: 240-247, 2007.
- 3) 中山泰秀, 辻中貴大, 岩井良輔, 松井悠一, 内田欣吾, 田地川 勉, 大場謙吉, 色素徐放による体内組織形成の爆発的加速化, *人工臓器* 40: S154, 2011.
- 4) Oie T, Yamanami M, Ishibashi-Ueda H, Kanda K, Yaku H, Nakayama Y: In-body optical stimulation formed connective tissue vascular grafts, "biotubes", with many capillaries and elastic fibers. *J Artif Organs* 13:235-240, 2010.
- 5) Watanabe T, Kanda K, Ishibashi-Ueda H, Yaku H, Nakayama Y: Development of biotube vascular grafts incorporating cuffs for easy implantation. *J Artif Organs* 10: 10-15, 2007.
- 6) Watanabe T, Kanda K, Ishibashi-Ueda H, Yaku H, Nakayama Y: Autologous small-caliber "biotube" vascular grafts with argatroban loading: a histomorphological examination after implantation to rabbits. *J Biomed Mater Res B Appl Biomater* 92: 236-242, 2010.